

Department of Thematic Studies  
Environmental Change

---

# Debris Flow Risk Mapping for Jämtland County, Sweden

*Nina Nkonge*

MSc Thesis (30 ECTS credits)  
Science for Sustainable Development

---



Linköpings universitet, SE-581 83 Linköping, Sweden

## Copyright

The publishers will keep this document online on the Internet – or its possible replacement – for a period of 25 years starting from the date of publication barring exceptional circumstances. The online availability of the document implies permanent permission for anyone to read, to download, or to print out single copies for his/her own use and to use it unchanged for non-commercial research and educational purpose. Subsequent transfers of copyright cannot revoke this permission. All other uses of the document are conditional upon the consent of the copyright owner. The publisher has taken technical and administrative measures to assure authenticity, security and accessibility. According to intellectual property law the author has the right to be mentioned when his/her work is accessed as described above and to be protected against infringement. For additional information about the Linköping University Electronic Press and its procedures for publication and for assurance of document integrity, please refer to its www home page: <https://ep.liu.se/>.

© 2024 Nina Gakii Nkonge

This work is licensed under the Creative Commons Attribution-NonCommercial 4.0 International License. To view a copy of this license, visit <http://creativecommons.org/licenses/by-nc/4.0/>



## Table of Contents

1. Abstract.....	1
2. List of abbreviations .....	1
3. Introduction.....	2
3.1 Objectives and Research Questions .....	4
4. Background and Conceptual Framework.....	5
4.1 What is a Debris Flow?.....	5
4.2 Debris Flow Preconditions.....	7
4.3 Risk .....	9
4.4 Critical Infrastructure (CI) .....	11
5. Study Area .....	12
6. Materials and Methods.....	13
6.1 Data extraction and pre-processing.....	14
6.2 Generation of a GIS Inventory of Critical Infrastructure (CI).....	16
6.3 DF Hazard Mapping .....	17
6.3.1 Slope .....	17
6.3.2 Soil type .....	18
6.3.3 Land cover .....	19
6.3.4 Aspect .....	19
6.3.5 Channel distance .....	19
6.3.6 Weighted Overlay Analysis .....	19
6.4 DF Hazard Susceptibility Validation .....	21
6.5 Identification of DF Risk to Critical Infrastructure (CI).....	21
6.6 Method Limitation .....	21
7. Results and Discussion .....	22
7.1 Results Validation.....	22
7.2 Debris Flow Susceptibility in Jämtland County .....	23
7.3 Conditions under which a Debris Flow is likely to occur in Jämtland .....	26
7.4 Debris Flow Risk to Critical Infrastructure in Jämtland.....	29
7.5 Study shortcomings and recommendations for future studies .....	34
8. Conclusions.....	36
9. Acknowledgments.....	38
10. References.....	39
11. Appendices.....	44

# 1. Abstract

The magnitude and frequency of debris flow (DF) are projected to increase globally and more so in the mountain regions. This is a result of increased precipitation which is associated with climate change. While rare, DFs severely impact critical infrastructure (CI) and society when they occur. Despite this, DFs are understudied in Sweden. This thesis aimed to bridge this knowledge gap by mapping DF risk in Jämtland County, Sweden. This was achieved using weighted overlay analysis to determine the susceptibility of the study area to DF hazards. Five DF susceptibility parameters were chosen (slope angle, aspect, soil type, land cover, and channel distance), reclassified on a scale of 1 to 5 (where 1 represented the lowest DF susceptibility and 5, the highest susceptibility), and then equal weights applied to produce the DF hazard output. The results show that Jämtland County has a *Medium* to *High* susceptibility to DF hazards. Particularly, the villages (or small towns) in the western parts of the county (Bakvattnet, Kallsedet, Åre, Duved, Undersåker, and Storlien) and the north (Ankarvattnet, Viken, Gäddede, and Valsjöbyn) are more susceptible to DF hazards. Besides, a DF hazard intersection with CI was carried out, indicating that about 57% of CI is located within the *Medium* DF hazard areas. In comparison, 32% is found within the *High* DF hazard areas.

**Keywords:** Critical infrastructure, Debris flow, Susceptibility mapping, Sweden, Weighted overlay analysis.

# 2. List of abbreviations

Abbreviation	Definition
CI	Critical Infrastructure
DEM	Digital Elevation Model
DF	Debris Flow
GIS	Geographic Information System
IPCC	Intergovernmental Panel on Climate Change
MSB	Myndigheten för Samhällsskydd och Beredskap (Swedish Civil Contingencies Agency)
RCP	Representative Concentration Pathway. The RCPs are named after the level of radiative forcing $W/m^2$ which is reached by 2100.
SIG	Statens Geotekniska Institut (Swedish Geotechnical Institute)
SGU	Sveriges Geologiska Undersökning (Geological Survey of Sweden)
SMHI	Swedish Meteorological and Hydrological Institute

### 3. Introduction

Climate change has contributed to increased extreme weather events globally and according to the Intergovernmental Panel on Climate Change (IPCC, 2023) global projections for the mountain regions, an increase in heavy precipitation (*high confidence*) will severely impact infrastructure, the economy, and society in the near future. When it comes to Sweden, the Swedish Meteorological and Hydrological Institute (SMHI, 2015) has projected that the future climate in Jämtland County will result in a precipitation increase of about 20% (RCP4.5) or 30% (RCP8.5) by the end of this century, depending on the emission scenario. Consequently, the country's mountain region is expected to experience increased frequency and intensity of landslides and debris flows (DFs) (Sweden's National Expert Council for Climate Adaptation, 2022).

Landslides and DFs are types of mass movements where a landslide falls under the "slide category" for mass movements whereas a DF is a "flow". While both involve the movement of material down a slope, the flowing nature of a DF means that there must be the presence of a liquid. That is, liquid (water from intense rainfall or snowmelt) and solid (earth material) forces must interact for a DF to happen (Iverson, 1997). On the other hand, a landslide involves the rapid sliding of earth material over one or more failure surfaces (Allaby, 2013). While recognising the severity and detrimental impact of other natural hazards, there is a dire need for detailed DF hazard and risk assessments. For one, DFs are very unpredictable often striking without warning, and can travel long distances due to their fluid nature. Besides, DFs can move very quickly with peak speeds exceeding 10m/s (Iverson, 1997). Also, DFs entrain material during motion making them very destructive along the flow path and depositional area (Iverson, 2014). This destructive power of DFs could destroy ecosystems, damage critical infrastructure (CI), and even endanger humans (Iverson, 1997; Jakob, 2005). For instance, a study conducted by Rheinberger et al. (2013) showed that in a 25-year period, DFs caused over 200 fatalities and more than £5 billion in economic loss throughout the European Alps. Similarly, Jakob's 2005 size classification for debris flows suggests that the smallest DF (size class 1) could potentially damage small buildings, size class 4 "*could destroy parts of villages, destroy sections of infrastructure corridors, bridges, ....*" while the potential consequences of the largest DF (size class 10) are "*vast and complete destruction over hundreds of km<sup>2</sup>*" (Jakob, 2005, p.155). The concept of CI is explained in detail in section 4.4, but in summary, CIs are assets or systems that are in place and are needed for society to function and whose failure could significantly impact society (MSB, 2014). Examples of CI include dams which are used for electricity production as well as water supply; airports, roads, and railways used for both private and public transport, food distribution, emergency services, among others; and electricity which is used for different services including residences, businesses, industries as well as in transportation.

Globally, there has been considerable attention on risk and hazard assessments around slope instability (this includes DFs, landslides, mudflows, among others). Some of these studies used DF instability factors to determine DF initiation zones and/or perform DF susceptibility mapping. For example, in their hazard assessment of potential periglacial DFs in the Swiss Alps, Kneisel et al. (2007) applied Geographic Information System (GIS) methods to identify DF initiation zones while Fischer et al. (2012) developed a framework for DF modeling aimed at susceptibility mapping in Norway and Niu et al. (2015) carried out a DF hazard assessment in China using rescaling and weighing methods. Other studies have mapped DF susceptibility using GIS and/or statistical methods (Esper Angillieri, 2020; Liang et al., 2020; Qin et al., 2022; Xu et al., 2013). More recent studies on natural hazards and risks in Sweden have mostly

focused on wildfires, floods, and landslides. As an example, Abbaszadeh Shahri et al. (2019) and Lindberg et al. (2011) conducted landslide susceptibility mapping in Sweden; Andersson-Sköld et al. (2013) did a landslide risk management, whereas wildfire hazards in Sweden were assessed by Johnsson & Balström (2021) and McNamee et al. (2022). This observation is consistent with the Swedish government's documentation on natural hazards. For example, Sweden's first climate-change vulnerability assessment identified flooding, erosion, and landslides as risks on roads and railways (Government of Sweden, 2007). Furthermore, the Swedish Portal for Climate Change Adaptation<sup>1</sup> has listed potential threats to the transportation infrastructure, among them, floods, storms, landslides, rising sea levels, and freezing conditions. These illustrations show that DFs are understudied in Sweden and there is a need to understand the basic processes affecting DFs (SGU, 2023). Moreover, the existing research on DFs as a climate-related hazard for Sweden is somewhat dated. Instances where such studies have been carried out include investigations on the geomorphological significance of DFs in the mountains south of Abisko, Northern Sweden (Rapp & Nyberg, 1981). Similarly, in a progress report as part of the research on *geomorphological processes and environmental changes in northern mountains*, Rapp (1995) reported several DF observations on grass-covered and blockfield slopes. Also, the need for further observations and mapping for improved warning systems was recommended by Nyberg & Rapp (1998) based on their discussion of rainfall-triggered debris flows during the summer and autumn seasons. Narrowing to those studies that have assessed the impact of climate change risks on infrastructure in Sweden, there appears to be no studies done for DF hazards. While Johnsson & Balström (2021) did a screening using GIS to identify climate change-related threats and impacts on road networks from wildfires, flooding, and landslides, Kalantari et al. (2014) applied a flood mapping method to assess the flood hazard along roads. No similar assessments have been done for DF hazards.

When it comes to the study area, a 2021 investigation of risk areas for landslides, erosion, and flooding in Sweden by the Swedish Geotechnical Institute [in Swedish, *Statens Geotekniska Institut*](SGI) and the Swedish Civil Contingencies Agency [in Swedish, *Myndigheten för Samhällsskydd och Beredskap*](MSB) highlights Jämtland County as a national risk area for slope instability. Furthermore, the Geological Survey of Sweden [in Swedish, *Sveriges Geologiska Undersökning*](SGU) has an ongoing task of mapping tracks from previous DF events (and other mass movements) in Sweden (Blomdin & Smith, 2021; SGU, 2024) and from the 2381 DF tracks that have already been mapped, 1600 tracks are in Jämtland county. This represents about 67% of the observations, a significant proportion given that DFs and other mass movements are likely to occur along paths from previous events (Blomdin & Smith, 2021; SGI, 2005). Besides, a DF occurred in Åre, Jämtland County, during the summer of 2023 as an aftermath of storm *Hans*, and severely damaged infrastructure (SGU, 2023). Moreover, the study area has very well-developed ski resorts with Åre frequently mentioned on several websites<sup>2</sup> as having the best ski resorts in Sweden. Therefore, informed by previous studies on hazard assessments around slope stability (Esper Angillieri, 2020; Fischer et al., 2012;

---

<sup>1</sup> Link to the Swedish Portal for Climate Change Adaptation: <https://www.klimatanpassning.se/en/effects/impacts-by-sector/transportation-1.166045>

<sup>2</sup> These websites were accessed on 06-06-2024 and include:

- Åre Sweden, link: <https://aresweden.com/en/alpine-skiing-in-are-ski-area/#:~:text=In%20total%20%C3%85re%20has%2042,in%20Scandinavia's%20largest%20ski%20resort>
- Fritiden.se, link: <https://www.fritiden.se/en/are/>
- Skiresort.info, link: <https://www.skiresort.info/best-ski-resorts/sweden/>
- Wikipedia, link: <https://en.wikipedia.org/wiki/%C3%85re>

Kneisel et al., 2007; Liang et al., 2020; Qin et al., 2022; Xu et al., 2013) and given the projected increase in precipitation (IPCC, 2023; SMHI, 2015), and consequently, increase in slope instability in Sweden's mountain region (SGI & MSB, 2021; SGU, 2023; Sweden's National Expert Council for Climate Adaptation, 2022), this study addresses a timely topic in Sweden: that other than wildfires, floods, and landslides which have received more attention in Swedish natural hazards research (Abbaszadeh Shahri et al., 2019; Andersson-Sköld et al., 2013; Johnsson & Balstrøm, 2021; Kalantari et al., 2014; Lindberg et al., 2011; McNamee et al., 2022), DFs are also significant hazards which can greatly impact society, therefore, the need for DF hazard and risk assessments. Furthermore, this study's assessment contributes to the achievement of the Sustainable Development Goals (SDGs) by directly addressing *target 11.b* which focuses on mitigation and adaptation to climate change as well as resilience to disasters in line with the Sendai Framework for Disaster Risk Reduction; and *target 13.1* focusing on strengthening resilience and adaptive capacity to climate-related hazards and natural disasters<sup>3</sup>.

### 3.1 Objectives and Research Questions

As highlighted in the previous section, debris flows in Sweden are understudied with research on climate-related natural hazards focusing mostly on wildfires, landslides, and floods. Where this research exists, it is somewhat dated and goes back to the 1980s and 90s. Therefore, this thesis addresses the identified research gap by focusing on Jämtland County, Sweden, with an overall aim of assessing and mapping debris flow risk to critical infrastructure in the study area. The results will support efforts to build a debris flow risk database in the study area, which can be scaled nationally. Secondly, information on areas under exposure to debris flow hazards will support decision-making processes and empower stakeholders in designing adaptation and mitigation strategies.

To achieve the aim of this study, the following questions are addressed:

- RQ.1: How susceptible is Jämtland to debris flow hazards and under what circumstances is a debris flow likely to occur in the area?
- RQ.2: To what extent are critical infrastructures in Jämtland exposed to debris flow hazards?

---

<sup>3</sup> Link to the United Nations SDGs and their targets accessed on 07-06-2024 via [https://sdgs.un.org/#goal\\_section](https://sdgs.un.org/#goal_section)

## 4. Background and Conceptual Framework

### 4.1 What is a Debris Flow?

A debris flow (DF) is a type of mass movement (also referred to as mass wasting). The Dictionary of Geology and Earth Sciences (2013) describes a mass movement/wasting as a process where earth material is transferred down a slope and these movements are grouped into four main categories: (i) flows (for example, a debris flow); (ii) slides (for example, a landslide); (iii) falls (for example, a rock fall); and (iv) creeps (for example, a soil creep). Different mechanics such as grain size, sediment concentration, shear strength, and flow speed have been used to explain DFs (Coussot & Meunier, 1996; Gregoretto et al., 2016; Iverson, 1997, 2014; Qin et al., 2022; Rickenmann, 1999; Vianello et al., 2023) and according to Iverson (1997), solid and fluid forces must interact for a DF to happen. These forces influence the DF mechanics. Hence, this thesis adopts Iverson's (2014, p.15) definition that DFs are “*water-laden masses of soil and fragmented rock that rush down mountainsides, funnel into stream channels, entrain objects in their paths, and form lobate deposits when they spill onto valley floors*”. Following this description, debris slides, debris torrents, debris floods, mudflows, mudslides, mudspates, hyper-concentrated flows, and lahars are qualified as DF events (Iverson, 1997). In Fig.1, an illustration of how a DF occurs is presented. Dissecting the term "debris flow", "debris" denotes the presence of sediments with varying grain sizes and irregularly shaped material. On the other hand, "flow" signifies an almost fluid movement during motion where the agitated debris is rearranged along the flow track (Iverson, 2014). Fig.1 shows the flow track while in Fig. 2A & B, the fluid movement along the flow track can be seen. Furthermore, a DF originates where the source area (Fig.1) meets certain preconditions. These preconditions are discussed in subsequent sections, but ideally, on steep slopes where there is low cohesion and/or loosely fragmented superficial deposits (Fig.1). As a result of intense rainfall or snowmelt, the superficial deposits get soaked and eventually, the internal frictional forces can no longer resist the driving forces hence being forced to move downslope (Iverson, 2014; Zimmerman, 1990). This marks the onset of a DF.

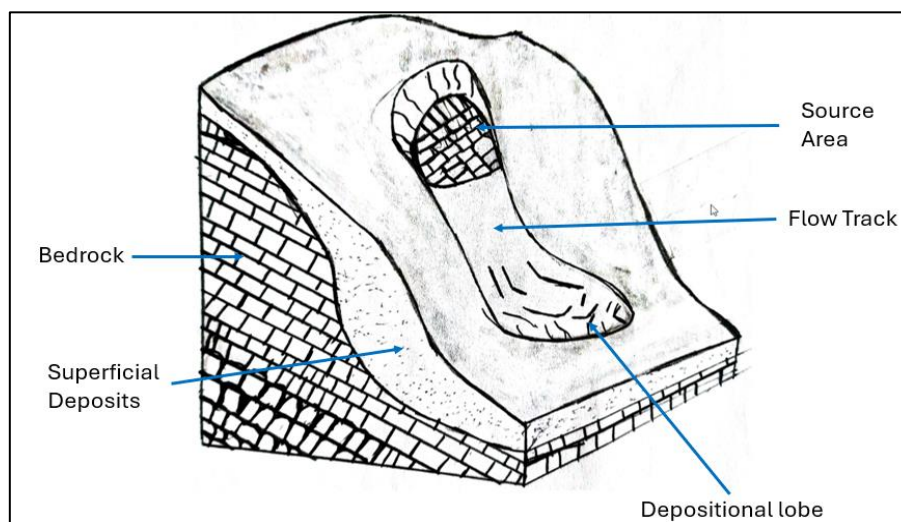


**Fig.1:** The morphology of a debris flow. Hand-drawn image by Austin Karani (2024) as a variation of Nettleton et al. (2005) original image<sup>4</sup>.

During motion, a DF grows in size as it captures more sediment along the flow track. This process is referred to as entrainment and could include scouring of bedrock material and even

<sup>4</sup> Original debris flow image accessed on 25-04-2024 under CC BY 4.0 license (<https://creativecommons.org/licenses/by/4.0/>)

trees in forested areas (Iverson, 2014). As seen in Fig. 2A&B, a DF vigorously moves downslope, occurring like “one or more unsteady and nonuniform surges” (Iverson, 1997, p.257). Eventually, depositional lobes (Fig.1) will be formed as a result of the reduced kinetic energy of the driving forces and frictional resistance of the coarse-grained debris (Iverson, 1997, 2014). Recent debris deposits are easily identifiable given their composition (in Fig.2C, a mix of big stones, trees, and finer sediments can be observed) and destructive nature (Iverson, 2014).



**Fig.2. A and B:** DF in motion. Screenshot images taken from videos captured during a DF event in Illgraben, Switzerland<sup>5</sup> (Observations by the Swiss Federal Institute for Forest, Snow, and Landscape Research). **C:** DF depositional area. The picture was taken in the Mörviksån catchment, Åre, Jämtland County after the summer 2023 DF event (Source, SGU, 2023).<sup>6</sup>

<sup>5</sup> Debris Flow motion images captured from a video on 12-04-24 via <https://www.wsl.ch/en/about-wsl/instrumented-field-sites-and-laboratories/experimented-field-sites-for-natural-hazards/feldbeobachtungen-und-datenerhebung/debris-flow-observation-station/>

<sup>6</sup> These pictures have been used with permission from the relevant authorities:

- Swiss Federal Institute for Forest, Snow, and Landscape Research: permission granted by Christoph Graf, a technical staff member of the debris flow project in the Illgraben, Switzerland.
- Sveriges Geologiska Undersökning (SGU): permission granted by Gustaf Peterson Becher who authored the *SGU-rapport 2023:11*.

## 4.2 Debris Flow Preconditions

This study understands DF precondition/s as factors that are already present and have the potential to initiate a DF. Principally, DFs are triggered by intense rainfall or snowmelt in steep slopes (Iverson, 2014) where there are poor runoff conditions and along previous DF paths (Blomdin & Smith, 2021; SGI, 2005). Moreover, SGI's study in 2005 established that for Sweden, areas with a likelihood of DF occurrence include slopes with an inclination greater than 17°, all gullies and torrents, slopes with poor vegetation cover, and areas with scars from erosion, landslides, and DFs. Further, most mass movements in Sweden occur in areas with clay and silt sediments, and also in slopes with till and coarse-grained sediments. This is based on previous studies where MSB continually maps areas with clay and silt sediments while the 2005 study by SGI established that slope instability could also occur on coarse-grained sediments (SGI, 2005).

Slope angle plays a big role in influencing the initiation of a DF event and is mostly used as the primary parameter in slope stability studies. Still, various pre-conditions including topographic (for example, slope angle, curvature, aspect); hydrological (for example Stream Power Index, channel distance), geologic (for example, soil type, distance from faults), land cover as well as human-induced factors (for example, distance from roads) have been used in previous research to investigate DF initiation/slope instability (Esper Angillieri, 2020; Fischer et al., 2012, Kanwal et al., 2016; Kneisel et al., 2007; Liang et al., 2020; Niu et al., 2015; Qin et al., 2019; Xu et al., 2013), and there is no defined criterion on which preconditions should be considered. As is seen in Table 1, the considered pre-conditions vary in number and type.

**Table 1: Debris flow pre-conditions used in various studies**

Parameter	Author/s					
	Esper Angillieri, 2020	Fischer et al., 2012	Kanwal et al., 2016	Qin et al., 2019	Xu et al., 2013	Current study
Aspect	X		X	X	X	X
Distance from drainage/proximity to a stream/channel distance	X		X		X	X
Distance from roads			X			
Distance from thrusts and faults			X	X		
Distance to road	X					
Elevation	X				X	
Land cover/ land use			X	X	X	X
Landforms				X		
Lithology/soil type	X		X	X	X	X
Melton ruggedness number	X					
Plan curvature	X	X	X			
Population density				X		
Precipitation				X		
Profile curvature	X					
Sediment transport capacity index	X					
Slope	X	X	X	X	X	X

Solar radiation	X					
Stream Power Index	X		X			
Terrain ruggedness index,	X					
Topographic position index	X					
Topographic Wetness Index	X		X			
Upslope catchment area for each DEM cell		X				
Vegetation coverage					X	

Precipitation is also key to the initiation of a DF and as such, this study assumes the presence of heavy precipitation as a criterion for a DF occurrence. In the previous section, it was explained that there must be the interaction of liquid and solid forces to initiate a DF (Iverson, 1997) and most DFs will be initiated following the onset of heavy precipitation (from intense rainfall and/or snowmelt) (SGI, 2005). In using precipitation to determine DF initiation, precipitation factors such as the intensity, duration, total amount as well as peak discharge should be considered (SGI, 2005). In Sweden, these precipitation factors are available from measurements taken by the Swedish Meteorological and Hydrological Institute (SMHI) measurements. However, this parameter is difficult to utilise given that most SMHI measurements are taken once a day, excluding data on short-duration rainfall (SGI, 2005). Besides, of the available SMHI stations, the highest concentration is in the southern part of the country leaving the northern and mountain areas with distances of about 60 km between stations (Alexandersson & Karlström, 2001 as cited by SGI, 2005). A representative precipitation data requires proximity to the study site, the same altitude, and that measurements are taken from the same side of the mountain (SGI, 2005). Therefore, this makes the daily average temporal and spatial resolutions for precipitation data in these parts of Sweden (including the study area) unreliable for this analysis. To confirm this, the SMHI website<sup>7</sup> was checked and it was found that for Sweden, precipitation data is available daily.

This thesis considered slope angle, soil type, land cover, aspect, and channel distance as the preconditions to analyse DF initiation. This decision was guided by the expertise of Swedish authorities, where previous studies by SGI and MSB (2021) have centred their analysis around slope gradient, land cover, and soil type. Besides, data availability for the different parameters also influenced the choice of the employed DF pre-conditions (for example, the unavailability of precipitation data, hence assuming its presence). Since these pre-conditions are used in DF hazard susceptibility mapping, this thesis refers to them as DF susceptibility parameters going forward. The DF susceptibility parameters used in this study are briefly highlighted below:

- **Slope angle** is an important factor in the initiation of a DF, where the steeper the slope, the more unstable. Different studies have determined the angle at which a DF is likely to be initiated, for example, slopes steeper than 17° (SGI, 2005); 25 - 30° (Iverson, 2014), and 30-45° (Delmonaco et al., 2003). However, some studies argue that slopes steeper than 36° will barely have any sediments since most of it has been removed, and as the steepness gets to 50°, the slope will mainly consist of rock (Nandi & Shakoor, 2010). This disparity could perhaps be attributed to other influencing parameters that come into play to cause slope instability and that these parameters differ spatially.

<sup>7</sup> SMHI website on precipitation information in Sweden. Accessed on 20-04-2024 through <https://www.smhi.se/en/climate/climate-indicators/climate-indicators-precipitation-1.91462#:~:text=SMHI%20has%20just%20over%20600,been%20used%20for%20this%20indicator.>

- **Soil:** The bulk density, cohesiveness, shear strength, particle size, and porosity of a given soil type influence the surface runoff (SGI, 2005). For instance, fine-grained soils such as clays and silts have a high plasticity index and are highly saturated with water hence increased pore pressure. This reduces their shear strength making them more susceptible to slope failure (Nseka et al., 2022).
- **Land cover:** In a slope where there is a dense cover of shrubs and trees, surface runoff is reduced hence increasing stability (Li & Duan, 2024; SGI, 2005). Furthermore, plant roots bind soils which increases their shear strength, consequently, making them less susceptible to slope failure (Li & Duan, 2024). On the other hand, land use-related activities such as agriculture and the construction of roads destroy the soil structure and vegetation, which increases the susceptibility to DFs (SGI, 2005).
- **Channel distance:** Slope instability occurs closer to streams as a result of the erosive processes within stream basins. This undercutting of banks affects adjacent areas with the susceptibility level reducing with increasing distance (Esper Angillieri, 2020; Kanwal et al., 2016; Nandi & Shakoor, 2010; Vianello et al., 2023). Besides, at distances greater than 200 metres, the susceptibility decreases because of a reduced supply of material (Rozos et al. 2008, as cited by Vianello et al., 2023).
- **Aspect** affects slope stability through its impact on moisture retention and vegetation, consequently impacting soil compaction (Raghuvanshi et al., 2015 as cited by Mekonen et al., 2022).

### 4.3 Risk

In the context of climate change, risk is viewed as either negative or positive consequences, where positive risk is seen as the potential benefits or opportunities that may arise from a climate-related event. This study adopted the IPCC general definition where risk is perceived as only the negative consequences, that is, the potential for adverse consequences in social-ecological systems (Reisinger et al., 2020). Further, the IPCC guides that risk is a consequence of the dynamic interactions between hazards, the exposed elements, and the vulnerability of the socio-ecological systems in question. Besides, this interaction could be a result of the potential impacts of the hazards and/or responses by society to these hazards (IPCC, 2019, p. 696). This dynamic interaction is illustrated in Fig. 3. The same report (p.688) describes a hazard as "*the potential occurrence of a natural or human-induced physical event or trend that may cause loss of life, injury, or other health impacts, as well as damage and loss to property, infrastructure, livelihoods....*". Similarly, exposure is described as "*the presence of people, livelihoods...infrastructure, or economic, social, or cultural assets in places and settings that could be adversely affected*" (IPCC, 2019, p. 685). In the context of this study, the scoped elements in the analysis were *DF Hazard*, *Exposure* and *Risk* (Fig.3). At first, to produce the DF hazard output for the study area, DF susceptibility parameters were used as inputs (aspect, channel distance, land cover, slope and soil type). Secondly, selected CIs were used as inputs to inform what elements are exposed to DF hazards in the study area (*Exposure*). The interaction where DF hazards and exposed CI intersect in the study area formed DF risk in Jämtland.

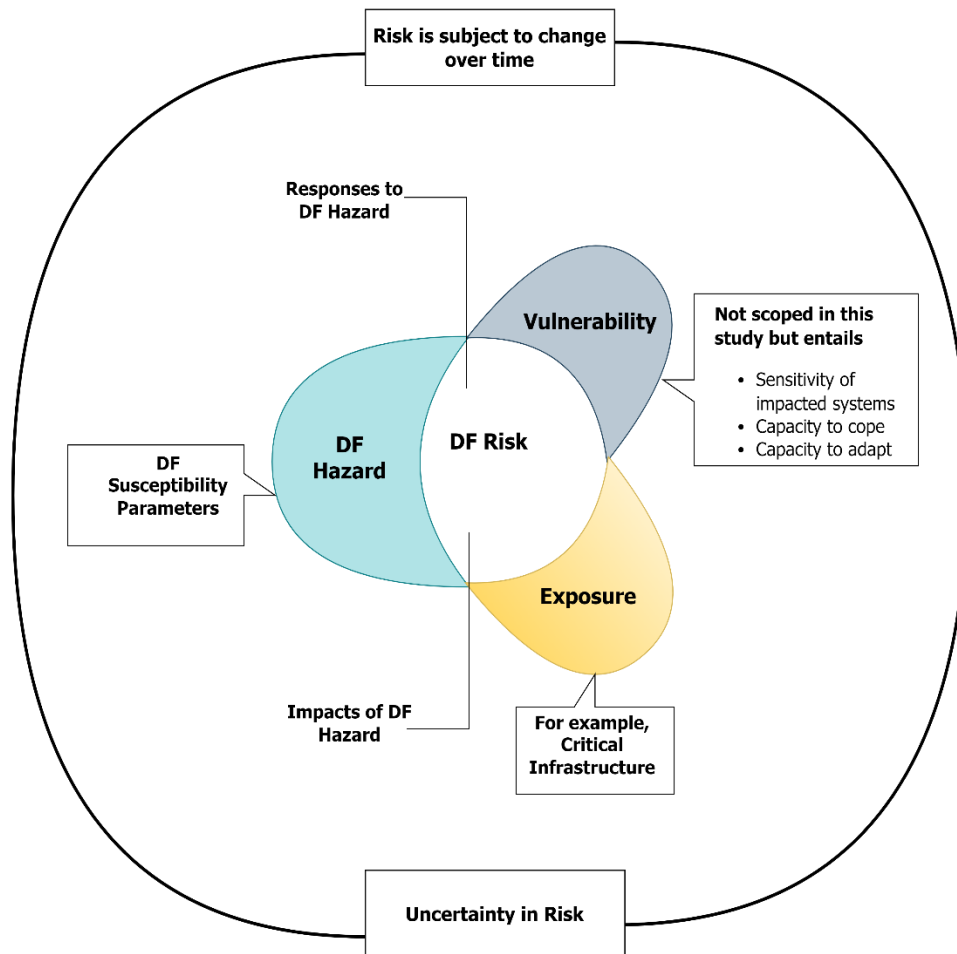


**Fig. 3:** An overview of how debris flow risk has been conceptualised for this study. Adapted from IPCC AR6 (2022).

This thesis recognises vulnerability as an important component in risk assessment where investigations need to be carried out to determine the susceptibility of involved systems to potential threats (IPCC, 2019). As such, conducting a vulnerability assessment would require examining preparedness in terms of the capacity to respond, cope, or adapt, which requires additional and extended quantitative and qualitative data sources. Therefore, given the limited time within which this study was conducted, vulnerability assessment was not scoped. In light of this, DF risk to critical infrastructure was contextualised as a product of DF hazard and the exposed critical infrastructure (Fig.3). Also, the specifics that would allow the quantification of DF hazards, for example, the magnitude of a DF, the scale, and its distribution, were not scoped in this thesis. Instead, DF hazard is characterised in terms of DF classes. These DF hazard classes (which later form the risk classes) are based on a qualitative risk ranking approach. In their *Guide to Risk and Vulnerability Analyses*, MSB (2012) discusses that the typical ranking scale should have five classes. This approach was adopted in this study where both DF hazard and risk were ranked into five classes (with their corresponding scales): Very Low (1), Low (2), Medium (3), High (4), and Very High (5). Where used, *Very Low* is an indication that the hazard is not expected to happen while *Very High* indicates that the hazard is very likely to occur. Interpreting this in terms of the impact, *Very Low* is an indication that the impact would be negligible while *Very High* indicates severe consequences. The other classes (*Low*, *Medium*, and *High*) should be taken as intermediate classes. Lastly, following IPCC’s risk framing, this study assumes that (i) there is uncertainty in the DF occurrence, hence uncertainty in exposure to DF risk; and (ii) the magnitude and DF risk in the study area can

change over time. This is in consideration of the dynamic interactions between the three aspects of risk (hazard, exposure, and vulnerability) where a change in one aspect can influence others (Fig.3).

#### 4.4 Critical Infrastructure (CI)

MSB's definition of CI is adopted where they describe CI as "*those assets, systems or parts thereof located in the European Union (EU) Member States which are essential for the maintenance of vital societal functions, health, safety, security, economic or social well-being of people, and the disruption or destruction of which would have a significant impact in a Member State as a result of the failure to maintain those functions*" (MSB, 2014, p. 12)<sup>8</sup>. MSB has identified eleven societal sectors within which CI can be identified: energy supply; financial services; trade and industry; health, medical and care services; information and communication; transport; municipal technical services; foodstuffs, public administration; protection, safety and security; and social security. The CI concept has been applied in previous research, for example, by Sonesson et al. (2021) who investigated how interdependency-related risks for three selected infrastructural sectors in Sweden (transport, communication, and energy) could be addressed. Also, Larsson & Grobe (2023) mapped the different data dimensions that are needed for critical infrastructure risk analysis in Sweden following MSB's concept of CI.

In the context of this study, CI mainly falls within three sectors, that is transport, energy supply, and municipal technical services. However, since there is a high interdependence in the functioning of CI to serve society (MSB, 2014), the other sectors might be impacted and an attempt to highlight these interdependencies will be made. Such high interdependence and the effects could be understood as cascading impacts (IPCC, 2019). The IPCC (2019) defines cascading impacts as the secondary events resulting from hazards that disrupt social-ecological as well as natural systems. Furthermore, *cascading impacts are complex and multi-dimensional and are associated more with the magnitude of vulnerability than with that of the hazard* (Pescaroli & Alexander, 2015 as cited by IPCC, 2019, p.680). Thus, in the context of this study, cascading impacts refer to a sequence of complex secondary consequences resulting from DF hazards and the interdependence that exists between exposed CI.

---

<sup>8</sup> This definition is based on the EU's Directive 2008/114/EC. The identification and designation of European critical infrastructures and the assessment of the need to improve their protection. European Parliament, Council of the European Union. Available at <https://eur-lex.europa.eu/eli/dir/2008/114/oj>

## 5. Study Area

Jämtland County [in Swedish, *Jämtlands län*] is located in Western Sweden at latitude 63.1712° N and longitude 14.9592° E (Fig.1). The highest point in Jämtland is 1796 metres (Syltoppen) while the lowest is 37 metres above sea level. As seen in Fig. 4, the Western part of the county is more mountainous (the elevation denoted by darker shades of green) while the Eastern part is more low-lying with basins and hills (the lighter shades in brown). Jämtland is the third largest county in Sweden measuring 49,443 km<sup>2</sup> and borders Norway on the West, Dalarna and Gävleborg Counties on the South, Västernorrland County on the East, and Västerbotten County on the North. Administratively, Jämtland has eight municipalities: Åre, Berg, Bräcke, Härjedalen, Krokom, Östersund, Ragunda and Strömsund. Given its surface area, Jämtland is a sparsely populated county with about 132, 572 inhabitants (SCB, 2023). Östersund municipal is the most populated (accounting for 48.9% of the county population), followed by Krokom (11.8%), then Åre (9.4%). The least populated municipality is Ragunda with a population of 5135 inhabitants (3.9% of Jämtland's population) (SCB, 2023).

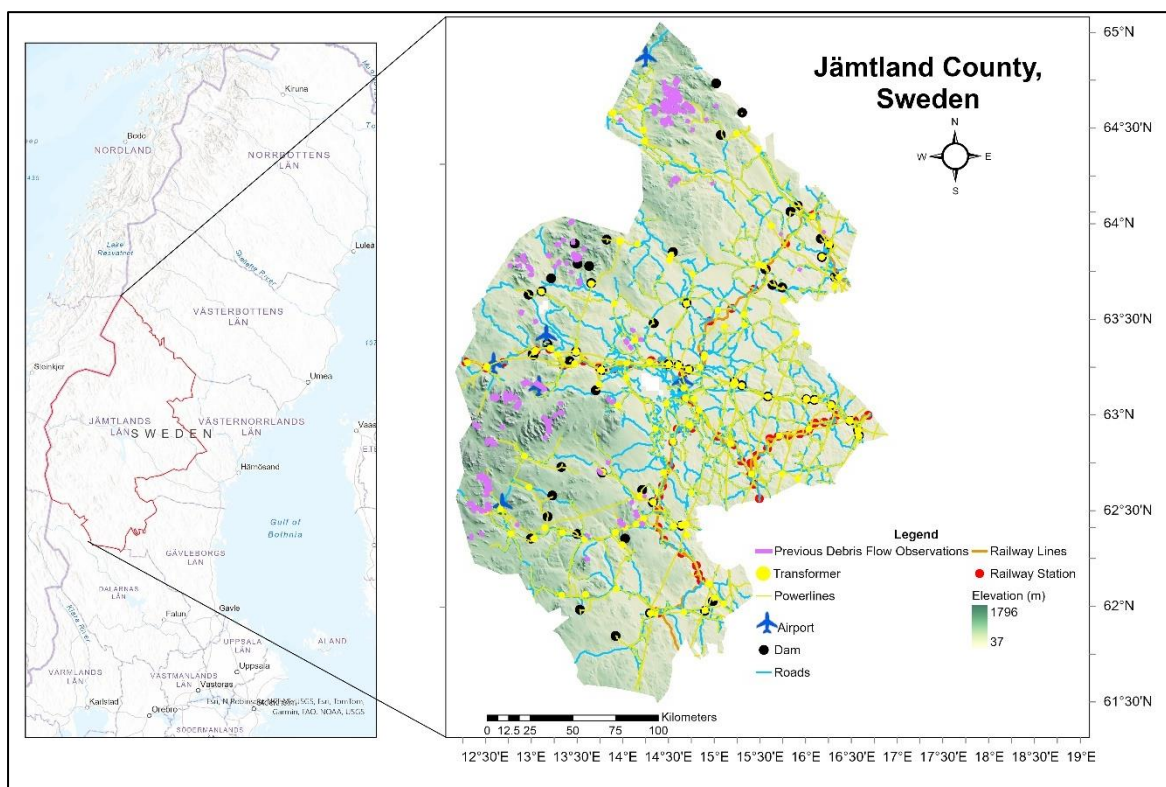


**Fig. 4:** Map showing the study area extent with some selected features.

The soil in the study area is mostly till, a soil type containing unsorted particles of clay, silts, sands, and boulders, and transported to the site by ice sheets. Parts of Jämtland have clayey and silty till. This type of till is made up of sedimentary rocks which are more erodible, therefore less blocks and more fine-grained soil (SGU, 2021). In terms of vegetation, the area is mostly forested with approximately 150-year-old spruce trees being dominant. Other tree species include pine, birch, willow, and aspen (Länsstyrelsen Jämtlands län, n.d.). Climate-wise, the Atlantic Ocean and Norwegian Sea have a high influence, especially during winter months which are rich in precipitation (with an average annual precipitation of about 1100mm). The coldest average winter temperature is about -11°C while in the summer, the maximum temperature averages at 14° (SMHI, 2023).

There are three railway network connections in the Jämtland: the *Inlandsbanan* which accommodates freight and summer tourist traffic; the *Atlantbanan* towards the western parts of the county and the *Norra Stambanan* passing through the eastern parts of the county. On the other hand, over 600 km of the national road network passes through the county, including two European roads: the *E14* from East-West (between Sundsvall and Trondheim) and the *E45* from South-North (between Gothenburg to Karesuando). Though not visible on the map (Fig.4), the electricity/powerlines are comprised of three levels: the main grid, regional grid, and local grid with the regional grid serving large consumers and the local grid. Finally, the county is served by two major airports, *Sveg* and *Åre/Östersund* (and other minor airports) with the latter being an international airport (Länsstyrelsen Jämtlands län, 2020), (Fig.4).

## 6. Materials and Methods

This study adopts the methodology from Hawchar et al.'s (2020) framework for high-level climate change risk assessment on critical infrastructure and is also inspired by other studies that have used GIS and/or slope instability methods (Esper Angillieri, 2020; Kanwal et al., 2016; Kneisel et al., 2007; Mekonen et al., 2022; Nandi & Shakoor, 2010; Niu et al., 2015; Qin et al., 2022; Vianello et al., 2023; Xu et al., 2013). These studies have used various slope instability factors to either identify landslide/DF initiation zones and/or perform susceptibility mapping and are used as reference points for example during the DF parameter reclassification: how these studies contribute to this thesis will be seen in the subsequent sessions. Hawchar et al.'s framework is a six-step process with critical infrastructure, climate threats, and climate change projections as input data (Hawchar et al., 2020, p.3). This study modified this framework into five steps with critical infrastructure and climate threats as inputs. In this case, the DF hazard (which is informed by various slope instability factors), was seen as the climate threat. The study methodology is illustrated in Fig. 5. A combination of ArcGIS Pro and manual processing of data in Excel was used for analysis. The steps and specific methods are described in the subsections below. Here, a clarification is made that the desired outcome of this study was not probability mapping, but rather, a mapping of DF susceptibility in the study area. This mapping followed a knowledge-driven approach by leveraging expert knowledge on slope instability to determine DF susceptibility (both by consulting current experts and literature).

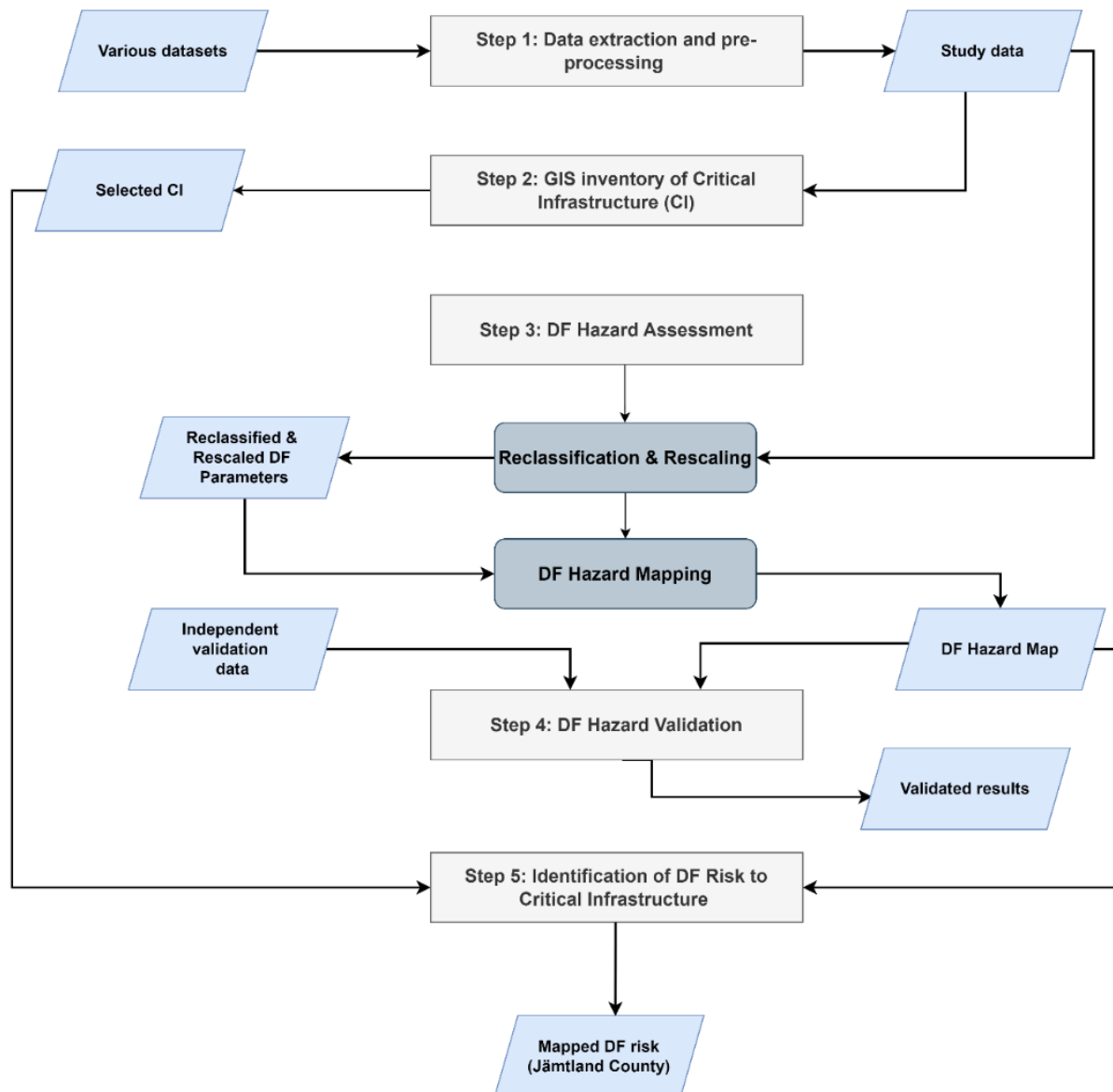


**Fig.5:** A high-level workflow illustrating the study methodology. The rectangles (light gray) signify the main steps, the rounded rectangle (dark gray) are sub-steps while the parallelogram (light blue) signifies a process input and /or output.

## 6.1 Data extraction and pre-processing

Data for this study was retrieved from different sources and is described in Table 2. Since the land cover dataset had a resolution of 10×10 metres, this study opted to resample the infrastructure datasets, soil types, dams, and the SGI and SGU validation datasets to this resolution. This was achieved by clipping the Swedish national elevation model using the Jämtland shape file and then resampling it to 10 metres. This output was used as the snapping input, a necessary step to ensure the same raster resolution and centre the pixels to the national elevation model (Süzen & Doyuran, 2004).

**Table 2: A description of datasets used in the study**

Dataset	Data description	Original name	Original data format	Source
Infrastructure and hydrography	Sweden's data on buildings, roads, railway lines, streams, among others	Topografi 10 Nedladdning, vektor	Shapefiles	Lantmäteriet. Link: <a href="https://www.lantmateriet.se/sv/geodata/vara-produkter/produktlista/topografi-10-nedladdning-vektor/">https://www.lantmateriet.se/sv/geodata/vara-produkter/produktlista/topografi-10-nedladdning-vektor/</a>
	powerlines & transformers	ledningar_In23		
	streams	hydro_In23		
	buildings	byggnadsverk_In23		
	facilities (including airport areas and runways)	anlaggningsomrade_In23		
	transportation including roads, railway lines, and railway stations	kommunikation_In23		
Soil types	Soil type data from Sveriges Geologiska Undersökning (SGU)	PRODUKT: JORDARTER 1:25 000-1:100 000	Shapefile	SGU. Link: <a href="https://www.sgu.se/produkter-och-tjanster/geologiska-data/jordarter--geologisk-data/jordartsdata/">https://www.sgu.se/produkter-och-tjanster/geologiska-data/jordarter--geologisk-data/jordartsdata/</a>
Land cover	Sweden's land cover data	Nationella Marktäckedata, nedladdningstjänst	Tiff	Swedish National Landcover Database (SDM). Link: <a href="https://geodatakatalogen.naturvardsverket.se/geonetwork/srv/swe/catalog.search#/metadata/0f1a86d5-d578-44bd-957e-3dcdb0b34ba0">https://geodatakatalogen.naturvardsverket.se/geonetwork/srv/swe/catalog.search#/metadata/0f1a86d5-d578-44bd-957e-3dcdb0b34ba0</a>
Dams	The dataset contains dams in Sweden	Dammar, Geografisk nivå: Nationell	Shapefile	Planeringskatalogen (Swedish power grid), 2022. Link: <a href="https://ext-geodatakatalog-forv.lansstyrelsen.se/PlaneringsKatalogen/GetMetaDataById?id=5b94e98e-9492-404a-84a1-5efab0c87599_C&amp;showmetadataview/">https://ext-geodatakatalog-forv.lansstyrelsen.se/PlaneringsKatalogen/GetMetaDataById?id=5b94e98e-9492-404a-84a1-5efab0c87599_C&amp;showmetadataview/</a>

Elevation	Sweden's National Height (NH) Model. The dataset contains elevation and hill shades at different angles.	Markhöjdsmodell Nedladdning, grid 1+	Tiff	Lantmäteriet. Link: <a href="https://www.geodata.se/geodataportalen/srv/swe/catalog.search;jsessionid=C62EDAC3543F83DEE269982F34D097C7#/search?resultType=swe-details&amp;_schema=iso19139*&amp;type=dataset%20or%20series&amp;from=1&amp;to=20&amp;fast=index&amp;_content_type=json&amp;sortBy=relevance&amp;or=grid%20%2B">https://www.geodata.se/geodataportalen/srv/swe/catalog.search;jsessionid=C62EDAC3543F83DEE269982F34D097C7#/search?resultType=swe-details&amp;_schema=iso19139*&amp;type=dataset%20or%20series&amp;from=1&amp;to=20&amp;fast=index&amp;_content_type=json&amp;sortBy=relevance&amp;or=grid%20%2B</a>
Jämtland boundary	The study area, created as a polygon	Search "Jämtlands län"	KMZ file	Google Earth Pro.
Sweden's municipal and county boundaries	Data clipped to the study area	Län, kommuner och LA-regioner, ArcView-shape (Zip-fil)	Shapefile	Statistics Sweden: <a href="https://www.scb.se/hitta-statistik/regional-statistik-och-kartor/regionala-indelningar/digitala-granser/">https://www.scb.se/hitta-statistik/regional-statistik-och-kartor/regionala-indelningar/digitala-granser/</a>
SGI dataset	Investigations of areas subjected to debris flow (used as validation data for the study).	karteringspunkt och områdesbegränsning"	Shapefiles	SGI, 2024. Investigations of areas subjected to debris flow. Hedfors J. <i>Personal communication.</i>
SGU dataset: debris flow tracks	Previously observed DFs in Sweden. For the study, the data is clipped to the study area (used as validation data for the study).	DF_lines_slamstromspar	Shapefile	SGU, 2024. Debris flow tracks (work in progress). Smith, C.A. <i>Personal communication.</i>

A study area slope map was then created from the elevation data using ArcGIS Pro analysis tools. The resulting slope output was used as input to create the study area aspect parameter. These outputs were used in section 6.3 as DF susceptibility parameters.

## 6.2 Generation of a GIS Inventory of Critical Infrastructure (CI)

As illustrated in Fig.5, after processing the study data, the next step was to generate an inventory of CI. At this point, infrastructure types from the transport, municipal technical services, and energy supply sectors were selected from the infrastructure dataset. This dataset had many data layers with each layer containing a large number of items representing various types of infrastructures, involving everything from buildings to construction lines and military protected areas. Therefore, to maintain a feasible focus during analysis, this study further limited the analysis items by focusing on the infrastructure types that are more critical for society's functionality.

Based on this, the following infrastructure of interest was extracted:

- roads - the seven biggest road types from the initial twelve were included. These are FreeRoad\_ExpressHighway[mötesfri väg], entrance /exit roads [infartsväg/utfartsväg],

county/regional roads [*landsväg*], overall link [*övergripande länk*], main/city streets [*huvudgata*], small country roads [*landsväg liten*], and small roads [*småväg*]. Smaller roads such as local streets [*lokalgata liten/ stor*] and neighbourhood roads [*kvartersväg*] were excluded.

- railway lines and stations (entire dataset).
- dams - three out of ten dam types that are infrastructure-related were selected (power production, water supply, and water management). Of the 57 dams present in the dataset, 32 are for power production while 25 are for water supply/management.
- buildings – to avoid data duplication, only the “main buildings” [*main.byggnad*] layer was selected from the available three building-related layers. The selected layer included most building types covered by the other two layers. For example, *church* as named in the “building point” [*main.byggnadspunkt*] layer is reflected as *community function* under the “main building” layer. Similarly, *sports field* and *recreation area* under “facilities” [*main.anlaggningsomrade*] layer are reflected as *other buildings* in the “main building” layer.
- Powerlines and transformers (entire dataset).

### 6.3 DF Hazard Mapping

As seen in Table 1, most common assessments of slope instability use a combination of influencing parameters to determine the same. This thesis achieved its DF hazard mapping by overlaying the DF susceptibility parameters (aspect, channel distance, land cover, slope, and soil type) using GIS overlay. An overview of how this was done is presented in one of the subsections below. Since the parameters had different types of values and units (continuous for slope, aspect, and channel distance; and categorical for soil and land cover), the ArcGIS Pro *Reclassify* tool was used to<sup>9</sup>:

- group data categories- this was the case for the land cover and soil parameters where the original classes were grouped into preferred classes and susceptibility factors applied to the new groups [Appendix 1 & 2; Table 3].
- reclassify and standardize the values to a common scale – this was applied to all the parameters as shown in Table 3. Five susceptibility classes with corresponding susceptibility factors were used, that is, *Very High* (with a susceptibility factor of "5"), *High* (4), *Medium* (3), *Low* (2), and *Very Low* (1). *Very High* was an indication that the given parameter class highly favours DF initiation while *Very Low* disfavours the initiation of a DF event. This step involved expert consultations to ensure accuracy in the exercise.

#### 6.3.1 Slope

To determine the most suitable slope angle for DF initiation in Jämtland County, the study area slope was initially categorised into five classes [0-5°, 5-12°, 12-30°, 30-45°, and >45°] and then this layer was overlaid against previous DF observations in Sweden (SGU dataset, 2024). The output showed that most DFs occurred at slope angles between 12-30° (69.8%), followed by 5-12° (19.1%), then 30-45° which accounted for 9.8%. About 1% of the previous DFs in the study area occurred at slopes between 0-5° and at slopes greater than 45°, the DF observations reduced accounting for only 0.2% of the observations. This output confirms Nandi

---

<sup>9</sup> ESRI documentation on ArcGIS Pro reclassification, accessed on 27-March-2024 through <https://pro.arcgis.com/en/pro-app/3.1/tool-reference/3d-analyst/an-overview-of-the-raster-reclass-toolset.htm>

& Shakoor's (2010) argument that the likelihood of a DF initiation will be reduced at very steep slopes since most material will already have been removed. Furthermore, according to Iverson (1997), fluid and solid forces need to interact for a DF to happen (based on this study's interpretation, at steep slopes, there will be reduced solid forces given that these slopes barely have any sediments). For this reason, this study assigned the class 12-30° the highest susceptibility factor, and the susceptibility factor was reduced for 30-45° and >45° classes (Table 3).

**Table 3: Reclassified Parameters alongside their DF susceptibility classifications and factors**

Parameter values	Parameter classification	Susceptibility Class	Susceptibility factor/ Rescaled value	Parameter classification	Susceptibility Class	Susceptibility factor/ Rescaled value
<i>Slope (Degrees)</i>				<i>Landcover</i>		
0 - 5	Very gentle slope	Very Low	1	Wetland, Water, Forested Wetlands	Very Low	1
5 - 12	Gentle slope	Medium	3	Forested	Low	2
12 - 30	Moderately steep slopes	Very High	5	Buildings	Medium	3
30-45	Steep slopes	Medium	3	Agriculture, Sparse vegetation, Exploited Land	High	4
>45	Very steep slopes	Very Low	1	Bare land	Very High	5
<i>Aspect</i>				<i>Soils</i>		
-1	Flat	Very High	5	Others	Very low	1
0 - 22.5	North	Very High	5	Boulders	Low	2
22.5 - 67.5	Northeast	Very High	5	Gravel, Others	Medium	3
67.5 - 112.5	East	Very High	5	Sand, Till, Others	High	4
112.5 - 157.5	Southeast	Very High	5	Silt, Clay, Organic Soils, Others	Very high	5
157.5 - 202.5	South	High	4	<i>Channel Distance (Metres)</i>		
202.5 - 247.5	Southwest	Medium	3	0-200	Very High	5
247.5 - 292.5	West	Very Low	1	200-400	High	4
292.5 - 337.5	Northwest	Low	2	400-600	Medium	3
337.5 - 360	North	Very High	5	600-800	Low	2
				>800	Very Low	1

### 6.3.2 Soil type

Soil classification was done following the Unified Soil Classification Systems (Casagrande, 1948) & SGU's *Tutorial for Geological Maps and Databases of Sweden* (SGU, 2021). However, some soil types could not strictly adhere to a classification based on particle size, and in such cases, the class "other" was devised to accommodate such exceptions. It should also be noted that the class "other" fell under different susceptibility factors depending on which processes formed the soil and where the soil occurs. For instance, soils that are not found on slopes were considered to have a very low impact since they are not associated with DF. On the other hand, soils resulting from slope and DF processes were considered to have a very high impact, hence a higher susceptibility factor. It is important to note that till is the most

common soil type in Sweden covering about 70 percent of the land (SGU, 2021). Given its high proportion, the assigned susceptibility factor for till is likely to significantly impact the results. The soil type “till” is composed of unsorted sediments transported by ice and for Sweden, the upper layers of the till consist mainly of sand and silt (SGU, 2021). Taking this into consideration, till was classified under the “*High*” susceptibility class. Still, some tills in Sweden are rich in clay and this type of till was classified under “*Very High*” susceptibility. This evaluation resulted in eight soil classes (from the original 51 classes) which were then rescaled on a scale of 1-5 [Appendix 1; Table 3].

### 6.3.3 Land cover

The original 20 land cover classes in the dataset were reclassified into nine classes based on the associated land covers in the study area (Li & Duan, 2024; SGI, 2005). Where the land is covered by wetlands/water or where it is a forested wetland, a DF susceptibility factor of 1 was assigned; where forested (2); buildings (3); where there is agricultural activities, sparse vegetation, or where the land is exploited (4); and where the land is bare, a DF susceptibility factor of 5 was applied [Appendix 2; Table 3].

### 6.3.4 Aspect

The aspect parameter and values were derived using the ArcGIS Pro *Aspect* tool which fitted the slope to ten classes. Guided by existing literature (Mekonen et al., 2022; Vianello et al., 2023), these values were reclassified into five classes with the flat, East, and North facing slopes receiving the highest DF susceptibility factor of 5 [Table 3].

### 6.3.5 Channel distance

Channel distance was created at intervals of 200 metres in ArcGIS Pro by creating five buffers on the stream layer (0–200, 200–400, 400–600, 600–800, 800–5000). The buffer intervals were according to Rozos et al. (2008) as cited by Vianello et al. (2023). Since it was not possible to input “>” using the *Multiple Ring Buffer* tool, the last class (800-5000m) was used as an indication of distances greater than 800m. These classes were then rescaled with those nearest to the stream receiving the highest susceptibility factor.

### 6.3.6 Weighted Overlay Analysis

After reclassifying and rescaling all the parameters, weighted overlay analysis was performed using the ArcGIS Pro *Weighted Overlay* tool. This tool facilitates the assignment of a percentage of influence to each raster input (in this case, the DF parameters). The weighted overlay formula is demonstrated below, and an illustrated example is shown in Fig. 6.

$$DF\ Hazard\ Score = (Sl \times 0.2) + (A \times 0.2) + (So \times 0.2) + (L \times 0.2) + (Cd \times 0.2)$$

Where *Sl* is the Slope, *A* – Aspect, *So* – Soil, *L* – Landcover, and *Cd* – channel distance.

The weighted overlay tool examines the cell values in each input raster, then these values are multiplied based on their proportion of influence and then the cumulative results produce the output raster (this further emphasises the importance of snapping the raster outputs to ensure the same resolution and cell alignment – explained in section 6.1).

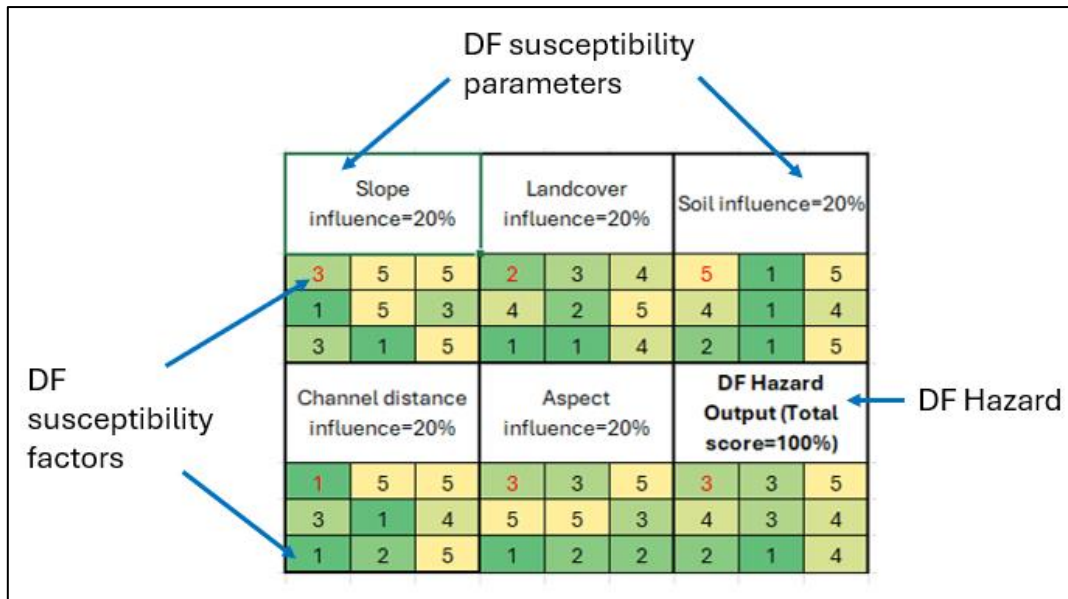


**Fig. 6:** A worked-out example of how the Weighted Overlay Tool in ArcGIS Pro works. The cell values are not actual (as per the project data) but assumed for purposes of demonstration. Illustration adapted from ESRI documentation<sup>10</sup>.

Using the illustrated example in Fig.6 and looking at the topmost values for each parameter from left to right (highlighted in red for ease of demonstration):

$$\{(3 \times 0.2 = 0.6) + (2 \times 0.2 = 0.4) + (5 \times 0.2 = 1) + (1 \times 0.2 = 0.2) + (3 \times 0.2 = 0.6)\} = 2.8$$

The output value is 2.8 but since the supported values are only integers, the result is rounded to the nearest whole number, in this case, 3, thus representing medium susceptibility to DF hazard. Different weighting methods are used in assessments involving composite indicators. Examples include principal component analysis (PCA), which assigns weights by aggregating variables, and equal weighting (Wiréhn et al., 2015). In this study, equal weights were applied (20% for each parameter) when carrying out the weighted overlay. An advantage of using equal weights for this kind of analysis is its fair assignment of the levels of influence. Using different weights implies that a given parameter has a stronger influence on DF initiation and, hence is given a higher priority. Given that there is a likelihood that the DF susceptibility parameters are interdependent (for example in the case where at very steep slopes soil is barely present), using other methods like PCA might over-emphasize some parameters (Brooks et al., 2005). Besides, assigning a parameter a higher weight would require evidence that the given parameter has a higher influence on DF initiation. This study did not come across such evidence.

<sup>10</sup> ESRI documentation on weighted overlay analysis accessed on 15-04-2024 through <https://pro.arcgis.com/en/pro-app/latest/tool-reference/spatial-analyst/weighted-overlay.htm#:~:text=The%20cell%20values%20are%20multiplied,1.5%20and%200.75%20is%202.25.>

## 6.4 DF Hazard Susceptibility Validation

Three datasets were used to validate the DF hazard output. These validations were not one-on-one comparisons, but rather, a check on how the different hazard classes overlay the observational datasets. These validation datasets are:

- *SGI Problem Areas*– these are built-up areas that SGI has identified as potential problem areas for DF, hence areas of interest.
- *SGI Mapped High Risks*- this is a mapping of areas that are prone to DFs and need further investigations to establish stability conditions.
- *SGU debris flow tracks* – this is a mapping of previously observed DF tracks in the study area (as seen in Fig.4). This dataset is part of ongoing work by SGU to update the geological information in Swedish northern and mountain regions. Once completed, this mapping will give an overview of how slope processes (landslides, debris flows, avalanches, rockfalls, among others) are spread in these regions (Blomdin & Smith, 2021).

Using this kind of validation gives confidence in the study results by checking the proportion of study results (in this case, DF Hazard estimations) overlaying observational datasets. This thesis could not find any study documenting what an agreeable proportion should look like, but ideally, having a high proportion of the observational datasets falling on the higher hazard classes would indicate high confidence in the results and, therefore successful DF hazard mapping. On the other hand, a high proportion of the observational datasets falling on the lower hazard classes indicates low confidence in the results and, therefore, a mismatch in the chosen method.

## 6.5 Identification of DF Risk to Critical Infrastructure (CI)

In the identification of DF risk to CI, Hawchar et al. (2020) point out the need to establish the relationship between climate threats (marked in Fig.5 as “*DF Hazard Map*”) and infrastructure types (marked in Fig.5 as, “*Selected CI*”), and where possible, development of an information matrix highlighting this relationship. Taking this into consideration, this study achieved this by:

- Creating a 100-metre buffer around the selected CI from section 6.2
- Merging the buffered infrastructure layers using the ArcGIS Pro *Merge* tool
- Extracting the number of pixels for each infrastructure type occurring in each hazard class (ArcGIS Pro *Extract by Mask* tool)

In this thesis, DF risk was assumed when the different hazard classes overlapped the 100 metres of the different CIs that were included in the analysis.

## 6.6 Method Limitation

Most of the data descriptions (ArcGIS Pro attribute tables) were in Swedish, and the pre-processing also involved translation (Swedish-English) of items of interest. Some meanings of less importance to the study might have been lost in the process and might have created potential sources of error, but utmost diligence was taken to ensure translation accuracy for the descriptions relevant to the analysis.

## 7. Results and Discussion

### 7.1 Results Validation

The DF susceptibility parameters in Jämtland were reclassified, rescaled, weighted, and overlaid using the steps described in section 6.3 to produce the DF hazard map for Jämtland County. The DF hazard output was then validated against three observational datasets as a way of increasing confidence in the study results, and also, to verify the reliability of the chosen study method. The results of this analysis are highlighted in Table 4. This validation approach has been employed in past studies. For example, in their landslide susceptibility mapping, Nandi & Shakoor (2010) overlaid their results against previous landslides in their study area and found that the highest proportion of previous landslides were concentrated in medium to high susceptibility classes (for their bivariate analysis) while 54% of the landslides were observed in the very high landslide susceptibility class (for their logistic-regression). Similarly, Vianello et al. (2023) did a comparison of their estimated DFs against documented DFs to assess which method had a better prediction capability. They argued that the method where most of the predictions fell within the high-extreme susceptibility was better in terms of prediction capability.

*Table 4: Debris Flow Hazard Validation Results*

DF Hazard Class	SGI Problem Areas		SGI Mapped High Risks		SGU Debris Flow Tracks	
	No. of pixels	%	No. of pixels	%	No. of pixels	%
Very Low	3262	0.19	10	0.05	0	0
Low	104326	5.97	977	5.31	213	0.47
Medium	832084	47.65	7376	40.09	8138	17.87
High	774926	44.38	9490	51.58	29605	65
Very High	31573	1.81	544	2.96	7587	16.66

Looking at the validation against the *SGI Problem Areas* (Table 4), the highest proportion of observations lie between the *Medium* and *High* DF hazard classes with the lower classes (*Low* and *Very Low*) accounting for about 6% of the observations. Given that about 94% of SGI's areas of interest can be observed in the *Medium*, *High*, and *Very High* DF hazard classes, is an indication that the hazard mapping is reliable. In the same way, the validation using the *SGI's Mapped High Risks* signifies alignment with this study's mapping (Table 4). Similarly, the SGU dataset was used based on the understanding that DFs (and other mass movements) tend to occur in places where similar events have occurred in the past (Blomdin & Smith, 2021; Nohani et al., 2019; SGI, 2005). Therefore, comparing how previous DF tracks (*SGU Debris Flow Tracks*, Table 4) overlay this study's DF hazard output indicates possible future DFs. Based on this validation, an almost negligible number of observations are seen in the lower classes with no tracks being seen in the *Very Low* class. On the other hand, combining the proportion of observations in the *High* and *Very High* hazard classes accounts for about 85% of the total observations.

## 7.2 Debris Flow Susceptibility in Jämtland County

The results show that Jämtland County has a *Medium to High* susceptibility to DF hazards with the northern and western parts of the county being more susceptible (Fig.7). Specifically, the towns or villages of Ankarvattnet, Viken, Gäddede, and Valsjöbyn in the north; and Bakvattnet, Kallsedet, Åre, Duved, Undersåker and Storlien in the west are located in areas where the DF susceptibility is higher. In the southern and eastern parts of the county, scattered pockets of *High* DF susceptibility can be observed.

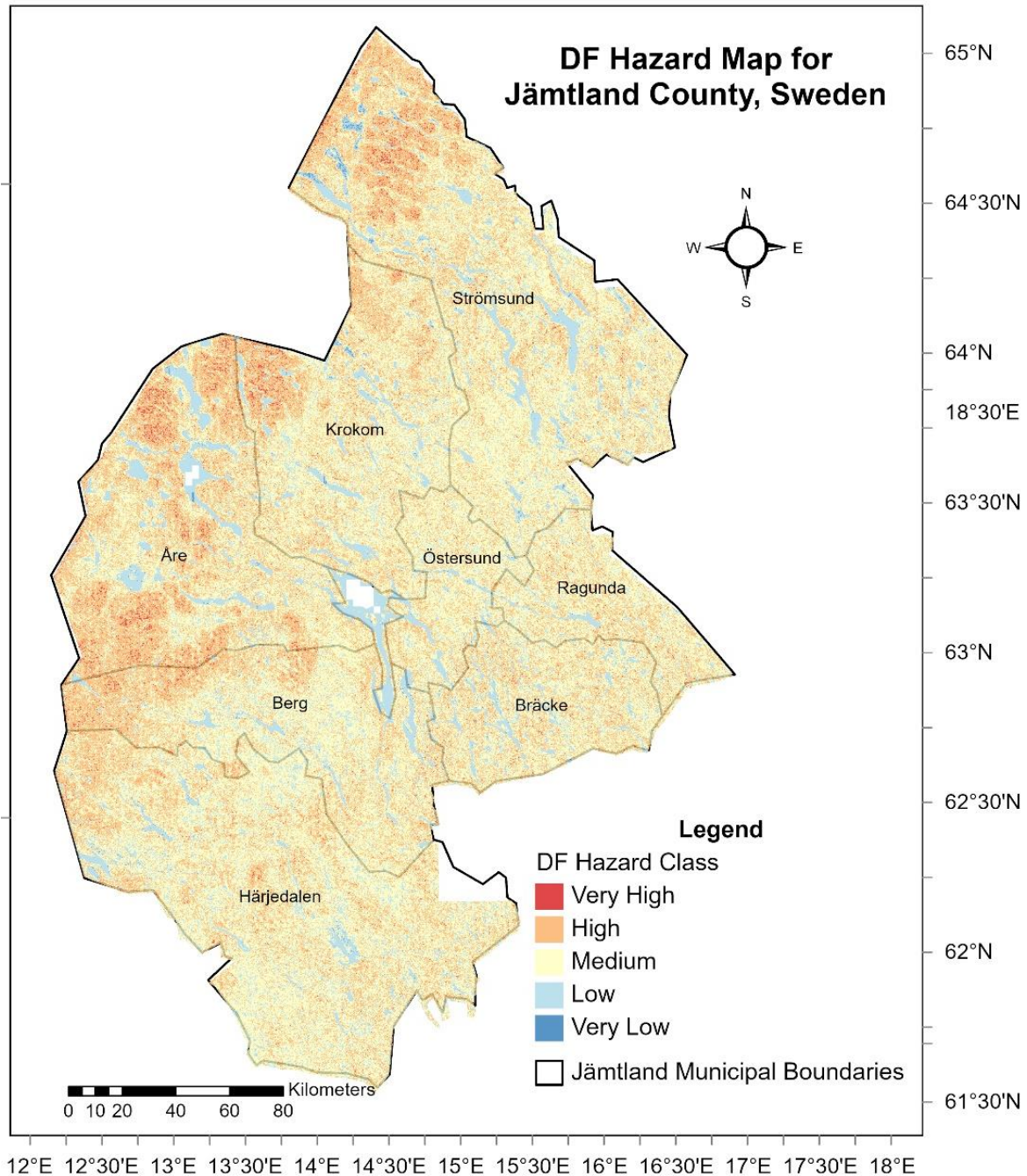


**Fig. 7:** A map showing the spatial distribution of debris flow hazard susceptibility in Jämtland County.

Overall, the *Medium* hazard class accounts for about 55% of the distribution, followed by the *High* hazard class (31%) and then the *Low* hazard class at 14%. The *Very High* and *Very Low* hazard classes are almost negligible, accounting for a combined total of about 1% (Fig.8). This high DF hazard susceptibility concentration in the western and northern parts can be attributed to slope angle, land cover, channel distance, and faults from previous DFs.

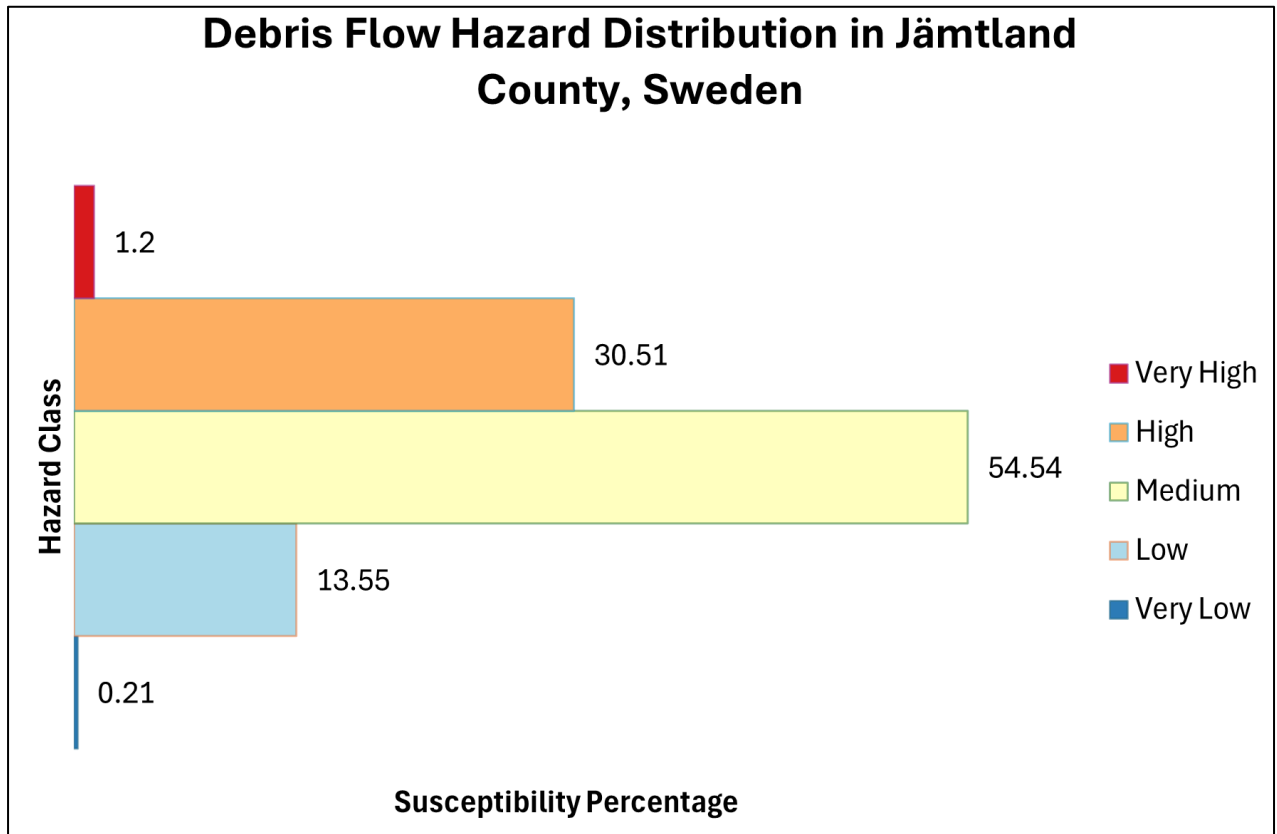


**Fig 8:** The distribution of DF hazard classes in Jämtland County, Sweden. The graph shows the percentage of the county's area under each hazard class.

On the other hand, the "*Very High*" susceptibility class for channel distance (between 0-200 metres), is almost evenly distributed throughout the county. Still, by carefully examining the parameter map, one can deduce that this parameter might have a great influence since very few pockets of the lower classes can be observed in the western and northern parts of the county (channel distance map in Fig.9). For the other two parameters (soil and aspect), it is not very obvious to identify their influence since the higher susceptibility classes for both parameters are evenly distributed in the county. In all the parameter maps in Fig. 9, the highest concentration of faults from previous DFs can also be observed in the northern and western parts of Jämtland. In contrast, the central part of Jämtland is characterised by either very gentle or very steep slopes which have a *Very Low* susceptibility to DF. These parts are also covered by forests and wetlands with a very small representation of other land covers (land cover map in Fig. 9). These observed patterns could probably be the reason for the *Medium* and *Low* DF hazard susceptibility in the central parts of Jämtland as seen in Fig. 7. How all this might influence DF hazards is discussed more in detail in section 7.2.

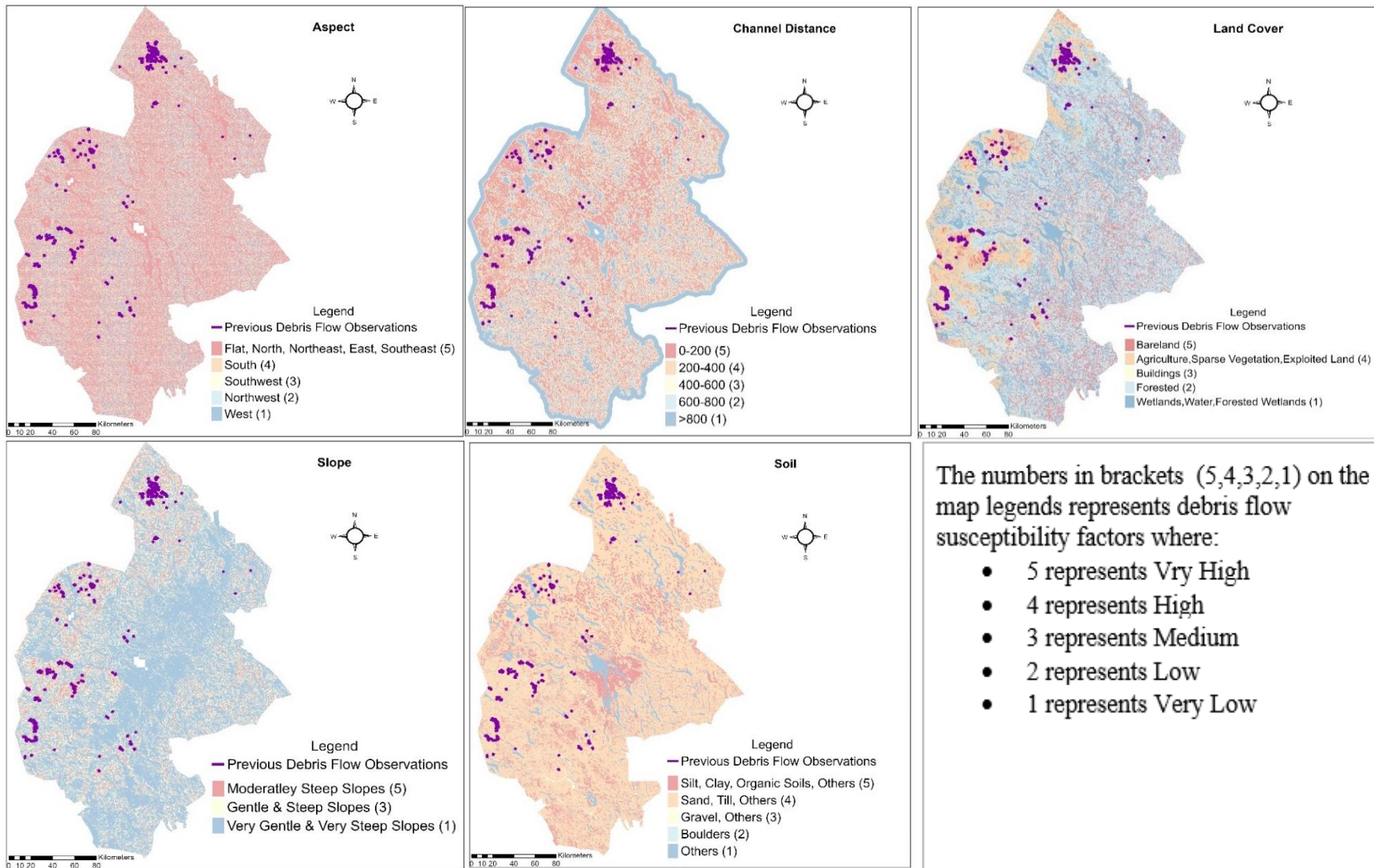


**Fig.9:** Maps showing observations of tracks from previous DF events (SGU dataset) against the different susceptibility parameters in Jämtland County.

The SGU dataset (highlighted in Table 2 and used in Table 4 as an observational dataset) was used to overlay the DF susceptibility parameters in this study. These outputs are seen in Fig.9. The findings in this study indicate that in Jämtland, DFs are likely to occur on moderately steep slopes (12-30°) that have disturbed soils (as a result of agriculture or exploitation from other land uses like road construction) or sparse vegetation, and where there is a dense concentration of waterways. By examining the parameters in Fig. 9, the northern and western parts have more moderately steep slopes (12-30°), a class that is very susceptible to DFs. When it comes to land cover, the “*High*” susceptibility class (agriculture, sparse vegetation, and exploited land) is mostly found in these parts of the county (Fig.9). Though not very concentrated, one can also see some bare land (shades of red in the landcover map in Fig.9), which is very highly susceptible to debris flow. Furthermore, given the high score in this study’s validation, the observations are to a large extent consistent with SGI’s 2005 study where in their report (p.12), they determined that in Sweden DFs (and landslides) occur in:

- “*slopes with soil cover and an inclination greater than 17 degrees*” – this is observed in this study. “slopes with soil cover” imply that the slopes cannot be very steep, otherwise the soil will have been removed.
- “*all gullies and torrents*” – this was not investigated in this study, thus, no observation for this was made.
- “*slopes with poor vegetation cover*” – this is confirmed in this study.
- “*areas with scars from erosion, landslides, and debris flows*” – this is also observed in this study.

### **7.3 Conditions under which a Debris Flow is likely to occur in Jämtland**

This thesis compares the impact of each DF susceptibility parameter using data on DF tracks (SGU dataset highlighted in Table 2) given that DFs (and other mass movements) are likely to occur along faults from previous events (Blomdin & Smith, 2021; Nohani et al., 2019; SGI, 2005). As is seen in Figs. 9 and 10, tracks from previous DFs are more apparent in some DF susceptibility parameter classes. These are, the *Very High* class for aspect (Flat, North, Northeast, East, and Southeast facing slopes); *Very High* class for channel distance (distances between 0-200 metres); *High* class for land cover (where land is covered by agricultural activities, sparse vegetation, or is exploited); *Very High* class for slope (moderately steep slopes, that is slopes angles between 12-30°); and the *High* class for soil (sand, till and others).

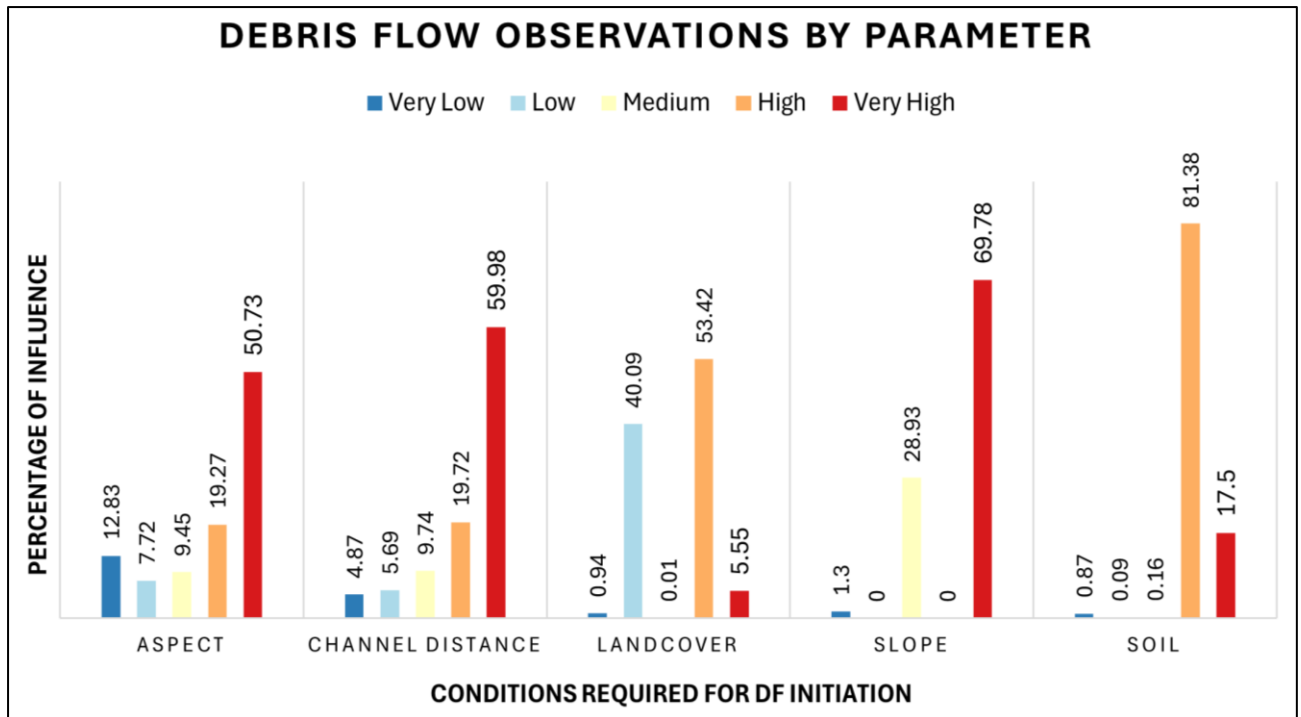


**Fig.10:** The distribution of debris flow tracks. This is observed for the different hazard classes per parameter.

Based on this comparison, there is a likelihood that DFs will occur where the slope is moderately steep (12-30°). By looking at Fig. 10, the highest proportion (about 70%) of DF tracks in Jämtland fall within the “*Very High*” susceptibility class for slope which corresponds to moderately steep slopes (slope map in Fig. 9). Also evident is the insignificance of very steep slopes (>45°) and very gentle slopes (0-5°). These two categories make up the “*Very Low*” susceptibility class which accounts for about 1% of the observations (Fig.10). Here, it is important to highlight that to improve the accuracy of the reclassification for the slope parameter, this study used the SGU dataset on tracks from previously observed DFs as basis to inform the various classes (this process is explained in more detail in section 6.3.1). As such, using the SGU dataset to inform the reclassification could explain the proportions of tracks observed for slope in this study. Importantly, the observations in this thesis for the slope parameter are consistent with those from previous studies. For example, a debris flow susceptibility mapping in Argentina by Esper Angillieri (2020) found most DFs to occur at slopes less than 20° and the significance reduced for slopes greater than 30°. Similarly, in his discussion of debris flow behavior, Iverson (2014) indicates that DFs occur at slope angles between 25-30° while SGI (2005) explains that for Sweden, DFs occur at slopes greater than 17° and that these slopes need to be covered by soil. This is an indication of slopes that are not very steep. This characteristic behaviour of slope angle’s influence on DF initiation can be partially explained by gravitational forces where at very gentle slopes, material is held in place, that is, little to no movement. On the contrary, as slopes become steeper, the shear stress (forces that pull material downslope) becomes stronger than the resisting forces holding the material in place (shear strength) hence causing movement (Nelson, 2013). Following this analogy of gravitational forces, at very steep slopes, material will already have been removed consequently little to no sediment availability (Nandi & Shakoor, 2010). Thus the explanation for minimal (if any) observations of DFs at very steep slopes.

Similarly, DFs are likely to occur where the land is covered by agriculture, sparse vegetation, and/or exploited (an example of exploited land is where roads and railways have been constructed). Based on the reclassification in Table 3, these land covers were assigned the *High* susceptibility class which as seen in Fig 10 accounts for 53% of the DF track observations. For one, trees intercept the amount of rain reaching the ground (Li & Duan, 2024). This affects surface run-off (SGI, 2005), consequently reducing soil saturation and pore pressure, hence increasing slope stability. Additionally, trees keep the soil in place by binding it through their root network (Gray & Sotir 1996 as cited by SGU, 2023). This would then explain the high observation of DF tracks in areas with sparse vegetation and/or where the vegetation cover has been removed for other anthropogenic activities such as grazing (agriculture) and construction. An interesting observation is the large proportion of DF tracks observed in the *Low class* (40%) and the small proportion in the *Very High class* (6%) (Fig. 10). These classes are represented by forested areas and bare land, respectively (land cover map in Fig.9). Given how trees might influence DF initiation (Li & Duan, 2024; SGI, 2005; SGU, 2023), this study expected to see a big proportion of DF tracks occurring where the land is bare and a small proportion where the land is forested. An explanation for this observation could be that Jämtland is mostly forested. Therefore, the chances of DFs occurring in forested areas would be large considering their great proportion in the distribution. Another explanation for this would be that in the study area, the land cover and associated land uses might have changed over time. As such, the areas that might have been forested when the DFs occurred could now be bare as a result of clear-cutting or other anthropogenic activities. The opposite could also have been the case, that is, the DF tracks could be from DFs that occurred during the Pleistocene time scale, that is before ice sheets retreated and melted in the study area. The study area covers what is discussed by Stroeve et al. (2016) as the central sector of the Fennoscandian ice sheet, a sector where deglaciation occurred 10.2 cal kyr BP (calendar years before the present). There are therefore chances that the forests in the study area did not exist then. These assumptions are worthwhile to investigate in future studies where for example, analyses could be centered on the impacts of land use (such as forest management or tourism-related activities) on DF initiation.

Looking at the soil map in Fig.9, it is not obvious to tell the influence of soil on DFs. As observed, the class “sands, till, and others” is found almost everywhere in the study area which can be explained by the fact that the study area is made up of mostly till (SGU, 2021). Nevertheless, about 81% of DF tracks are observed in this susceptibility class (marked as “*High*” in Fig.10). On the contrary, only about 18% of DFs are observed in the “*Very High*” susceptibility class which represents silts, clays, and organic soils (as seen in the soil map in Fig.9). This, together with the landcover classification discussed above, is probably the reason why there is a mismatched correlation between the DF susceptibility score for the “*Very High*” class and the observations. A possible explanation for the high DF susceptibility found in sands is that unconsolidated soils such as sands have low cohesion (the stickiness of material) hence promoting slope instability since such material covering the slope is weak (Nelson, 2013). Besides, the tills found in Jämtland are made from easily erodible sedimentary rocks, hence less blocky and more clayey (SGU, 2021). These tend to mimic the high plasticity observed in clays which promote slope instability (Nelson, 2013). Comparing the soil influence on slope stability with other studies, a landslide susceptibility mapping in southwest Sweden by Abbaszadeh Shahri et al. (2019) showed that most slope instability occurred in clays followed by sands. On the other hand, a debris flow hazard assessment in Italy found that slopes are more unstable on sedimentary rocks since they tend to promote the formation of superficial deposits (Delmonaco et al., 2003). The findings by Delmonaco et al. (2003) are consistent with this study's findings which observe more DF tracks in the *High* susceptibility class. This class represents sands, till, and others, where “others” include mountain bedrock, calcium-rich soils,

weathered soils, and sedimentary bedrock/soils (Appendix 1; soil map in Fig.9). Future studies could perhaps re-investigate the susceptibility of these two classes, that is, “*Very High*” (representing clays, silts, and organic soils) and “*High*” (representing sands, till, and others).

When it comes to channel distance, most DFs are seen to occur at distances between 0-200 metres (channel distance map in Fig. 9). This class is classified as *Very High* in terms of DF susceptibility and accounts for about 60% of the observations (Fig.10). The proportion drastically reduces for distances over 200 metres where the class *High* (200-400 metres) accounts for about 20% of the observations and as the distance increases to above 800 metres, only about 5% DF tracks can be observed. Similar observations were made by Esper Angillieri (2020) and Nohani et al. (2019) who found the largest influence on instability to have occurred within a distance of 100 metres from waterways. This occurrence of DFs in proximity to water channels happens because of erosive processes where streams erode their banks (through the process of undercutting) promoting instability (Esper Angillieri, 2020; Nandi & Shakoor, 2010; Nelson, 2013). Distance from waterways also affects soil moisture which reduces with distance (Nohani et al.,2019). The more the soil moisture, the more unstable a slope will be.

Lastly, the *Very High* susceptibility class for aspect accounted for 51% of the DF track observations (Fig.10). This class comprises the flat, North, Northeast, East, and Southeast-facing slopes (aspect map in Fig.9). The large proportion of observations in this class could be attributed to the combination of the five aspect categories. For this reason, this study’s outcome cannot explicitly determine the level of influence on DF initiation from these aspect categories (flat, North, Northeast, East, and Southeast). Future studies could perhaps attempt a different reclassification where these aspect categories are not grouped, but rather, examined individually. Nevertheless, some studies, for example, Esper Angillieri (2020) observed more DFs occurring on East and North-facing slopes while Mekonen et al. (2022) observed more DFs on East and Southeast-facing slopes. Thus, the observations of these two studies are somewhat consistent with what this thesis observes for aspect influence on slope stability. As explained by Vianello et al. (2023) the direction in which a slope faces will affect the slope’s solar exposure thus impacting vegetation and soil moisture retention ( Esper Angillieri, 2020; Raghuvanshi et al., 2015 as cited by Mekonen et al., 2022).

## **7.4 Debris Flow Risk to Critical Infrastructure in Jämtland**

This thesis presents a risk analysis by evaluating the existing CI exposed to DF hazards in Jämtland. The intersection of DF hazard areas with CI is shown in Figs. 11A and B while the distribution of the exposed CI to DF hazards is illustrated in Fig.12. In Jämtland, the western part of the county (covering most of Åre Municipality and some areas in Krokoms and Berg municipalities) is more susceptible to DF hazards but these areas have a lesser concentration of CI (Fig. 11A). Nonetheless, roads, railways, and electricity can be observed passing through the high-hazard areas. Buildings can also be observed in these areas (Fig.11A). On the other hand, CI in Jämtland is concentrated in the central and eastern parts of the county which are characterised by *Medium* DF hazard and some pockets of *High* DF hazard (Fig.11B). These areas include the entire extent of Ragunda and Östersund municipalities; parts of Berg, Bräcke, Krokoms, and Strömsund municipalities; and a very small part of Åre municipality.

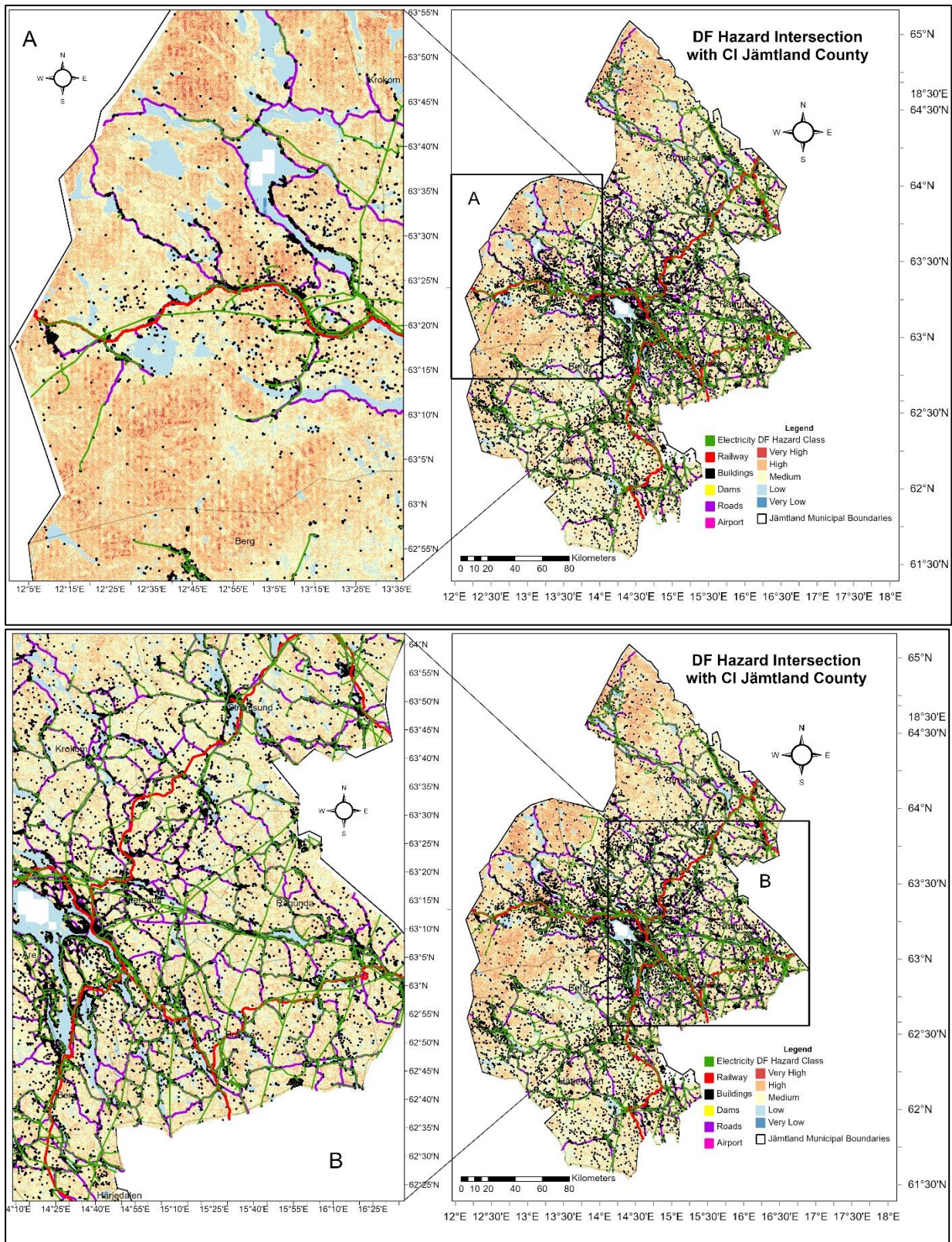


**Fig. 11:** DF hazard intersection with CI in Jämtland County. “A”: zoomed-in area highlighting where DF hazard susceptibility is higher. This area includes almost the entire extent of Åre Municipality (except a small portion towards the southeast of Åre) and small parts of Krokoms and Berg Municipalities. “B”: a zoomed-in area highlighting where CI is more concentrated. This area includes the entire extent of Ragunda and Östersund municipalities; parts of Berg, Bräcke, Krokoms, and Strömsund municipalities; and a very small part of Åre municipality.

As seen in Fig. 12, 89% of all CI included in the analysis is located in areas with *Medium-High* risk exposure. This is particularly problematic since these two classes align closely with the historical DF observations from SGU and risk mapping from SGI (validation results in Table 4). Besides, Jämtland is a national risk area for slope instability in Sweden (SGI & MSB, 2021), and this was affirmed when a debris flow occurred in Åre locality during the summer of 2023. This DF event greatly impacted society and direct consequences included damaged buildings and the closure of roads (SGU, 2023).

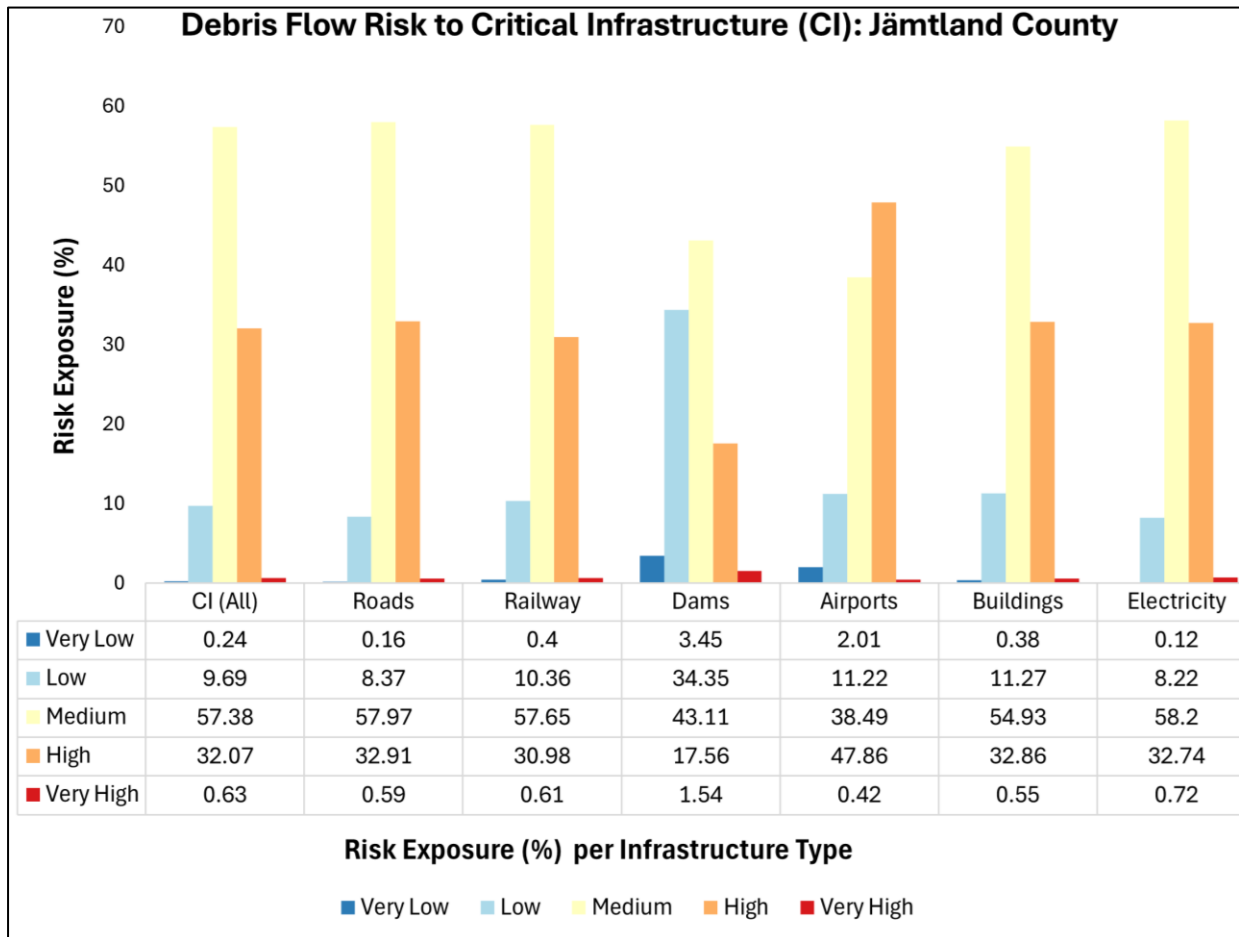


**Fig. 12:** Distribution of debris flow hazard intersection with Critical Infrastructure in Jämtland County.

This study identified the transport, energy supply, and municipal technical services as the sectors to which the study’s chosen CI belongs. However, a failure in one infrastructure type is likely to have cascading impacts (see section 4.4) (IPCC, 2019) where other infrastructures are affected and, consequently, other sectors and societal functions. Putting this into context, about 33 % and 58% of the electricity supply (power lines and transformers) for Jämtland are located in the *High* and *Medium* DF hazard areas. This means that the power supply in the county is highly exposed to failure in the event of a DF happening. According to the County Administrative Board in Jämtland (2020), about 40% of Sweden’s power outages are weather-related, and for Jämtland, the likelihood of slope failure (including DFs) could highly disrupt the power supply through damaged power lines and substations. The cascading impact of this would be the likely failure of the railway, which is very dependent on electricity. Electricity failure would also highly likely affect the Health, Medical, and Care Services sector as well as electricity usage in other businesses and residential buildings.

Similarly, dam failure is likely to directly affect the Energy sector through the production of electricity (MSB, 2014). In their risk and vulnerability analysis, the County Administrative Board in Jämtland County (2020) identified dam failure (specifically, power production dams) as the risk that would have the greatest societal consequences given that Jämtland produces 5–10 % of Sweden’s electricity. As such, dam failure would not only cause a local crisis but also impact the national level (Länsstyrelsen Jämtlands län, 2020), thus disrupting the county's and national electricity distribution. Besides the production of electricity, the dams in Jämtland also belong to the Municipal Technical Services sector through the supply of drinking water (MSB, 2014). Consequently, a DF event is likely to directly impact the water supply in the county with the cascading impacts being consequences on the Health, Medical, and Care Services sector and the Food sector (water is for example needed in the semi-processing of foodstuff, in restaurants, among others). These impacts can be demonstrated through a previous study by Koks et al. (2022) where they documented how critical infrastructure was impacted by the 2021 Western European flood event. The authors reported that in Bad Münstereifel, Germany, there was no connection to the fresh-water network for about five days, and after reconnection, the residents had to boil the water before consumption for about one month. Similarly, about 105 general practitioner practices were unable to operate as a result of a lack of running water and/or electricity (Ärzte Zeitung, 2021, as cited by Koks et al., 2022). As seen in Fig.12, about 43% and 18% of dams in Jämtland are located within the *Medium* and *High* hazard levels if a DF were to occur. Despite the dams in Jämtland being highly exposed to DF hazards, Svenska Kraftnät (2023, p.132) places “*heavy rainfall, snowmelt, and extreme floods*” as their focus areas for dam safety concerning climate change and environmental adaptation. This study interprets this to mean that other natural hazards such as mass movements that might result from the changing climate, have not been considered by Svenska Kraftnät in their dam safety assessment. Taking the DF susceptibility in the area and climate change into account, this thesis highly recommends that further investigations by Svenska Kraftnät and other relevant stakeholders are needed to determine the resilience of these dams in a DF event.

Next, to illustrate how a DF hazard could potentially impact society, this study demonstrates impacts on, and from the transport sector. The 2022 study by Koks et al. documented that about 600 km of railway tracks were destroyed in Germany during the 2021 floods in Western Europe, with an estimated asset damages of about 1.3 billion euros. This took the German railway provider (*Deutsche Bahn*) about six months to repair nine of the fourteen affected railway lines and two years to make all operational (Munchow, 2021 as cited by Koks et al., 2022). Similarly in Belgium, 10 km of railway tracks and 3000 sleeper tracks were destroyed with estimated costs of repair at about 30-50 million euros (Rozendaal, 2021a as by Koks et al., 2022). Similar impacts in the event of a DF could potentially occur in the study area. The railway network in Jämtland (highlighted in Fig.4; also, in Figs. 11A & B) is used for the transportation of goods and services (freight traffic), tourist traffic and also connects the county to other parts of Sweden (Länsstyrelsen Jämtlands län, 2020). Similarly, apart from the smaller roads that serve the county, Jämtland has national roads passing through the county, including the E14 and E45 (Länsstyrelsen Jämtlands län). About 58 % and 31 % of both infrastructure types (railways and roads) are located within the *Medium* and *High* DF hazard areas respectively (Figs.11 and 12). On the other hand, about 38% of the airports are found in the *Medium* DF hazard areas while 48% are within the *High* hazard areas. This, like other illustrations above, is taken to mean that in Jämtland, the Transport sector is highly exposed to DF hazards. Going back to how a DF deposition area could look (Fig.2C), it is possible that a DF could potentially lead to the closure of roads and railway sections. This image in Fig.2C shows an area that is upstream of a railway section on the eastern side of Mörviksån (in Åre

Municipal, Jämtland County) and downstream of E14 (SGU, 2023). Besides, this DF event also eroded the ski road from Sadeln and the ski bridge to Tott (SGU, 2023). If a DF were to occur in airport areas, airport runways, and buildings could potentially be impacted. Using examples from MSB (2014), disruptions in the transport sector could have cascading impacts on other sectors like the Information and Communication sector (for example, distribution of mail); Health, Medical, and Care Services sector (as seen in emergency medical services, pharmaceutical and equipment supply, transport of lab samples and care services); the Protection, Safety and Security sector (for example, police services, fire & rescue services, guarding and security activities, among others) and the Food sector through food distribution. Notably for the Food sector, disruptions in the Transport sector could potentially lead to food shortages in Jämtland given that no food manufacturing takes place in the county. Likewise, there are no wholesale warehouses within the county, and all food sold in grocery stores is transported in the county (Länsstyrelsen Jämtlands län, 2020).

To discuss the impact of DFs on buildings, this thesis highlights how other natural hazards have impacted buildings. For example, a study by Johansson (2015) recorded that during a 2012 flooding event in Småland, Sweden, basements flooded in about 100 private houses, also, in Nyköping City Hospital. Similarly, following the Western European 2021 floods, the basement, outbuildings, and entire outdoor area of a hospital were flooded in Eschweiler, Germany. This also caused the power supply to collapse and destroyed the building technology, resulting in the evacuation of 300 patients using helicopters. It took the hospital about four weeks to be partially operational and three months to be fully operational (SAH Eschweiler, 2021 as cited by Koks et al., 2022). Besides, the 2023 DF event in the study area also impacted buildings, for instance, the sedimentation (silt, sand, and gravel) witnessed at Åre old church (SGU, 2023). Lastly, the impacts on buildings following a DF event can be likened based on Jakob's (2005) ten-size classification for debris flows. In this classification, the smallest debris flow which is size class 1 (with a volume of 10 to  $10^2$  m<sup>3</sup>) could potentially damage small buildings; class 3 ( $10^3$  to  $10^4$  m<sup>3</sup>) could damage larger buildings; size 4 ( $10^4$  to  $10^5$  m<sup>3</sup>) could destroy parts of a village while size 6 ( $10^6$  to  $10^7$  m<sup>3</sup>) could destroy towns. If buildings are hit by a DF, cascading impacts would be for example effects on operations/services in those buildings which could vary from residential services, to medical and financial services, among others.

Sweden's Adaptation Communication (2022) identifies threats to society, infrastructure, and businesses from landslides, mudslides, and erosion among the priority areas for climate change adaptation. As a prerequisite for any adaptation plans, the identification of risk areas is necessary (Government Offices of Sweden, 2022; Iverson, 2014; Reisinger et al., 2020). This study has attempted this by mapping the DF hazard distribution in Jämtland County. The illustrations in this section on impacts are not actual investigations, but rather indications of how a DF hazard would potentially impact the critical infrastructure in Jämtland and, consequently, the society. It is therefore important that the relevant authorities carry out further investigations that would for example determine the coping capacity of the exposed infrastructure in the event of a DF happening (going back to the conceptual framework in section 4.3, this represents vulnerability analysis which was not scoped in this study). Besides, the construction of new infrastructure in Jämtland should take into account the area's susceptibility to DF hazards. Apart from this, it is fundamental to establish the interdependencies that exist between the identified CI, the sectors they belong to, and the societal functions they serve (MSB, 2014).

## 7.5 Study shortcomings and recommendations for future studies

DF hazard mapping is a challenging exercise given that DFs are triggered by the interaction of several complex susceptibility parameters. This variation and complexity in the susceptibility parameters to employ in a study is illustrated in section 4.2 and Table 1. As such, there is a need to ensure that the parameters that have the most influence have been considered. Usually, the parameters that influence slope instability can be grouped into geological (for example, soil type, soil texture, and faults from previous events), topographical (for example, slope angle, curvature, and aspect), hydrological (channel distance, stream power index), and land cover. Though this study only used five parameters (slope angle, soil type, land cover, aspect, and channel distance) an attempt was made to ensure that all categories were considered. Using fewer susceptibility parameters (in comparison to previous studies and as illustrated in section 4.2) might have affected the hazard mapping outcome, but to ensure authenticity in the chosen mapping method and results, validation was performed as described in section 6.4 and discussed in section 7.1.

Also, it is difficult to settle for a hazard mapping method given that each method presents its strengths and challenges. This thesis considered a weighted overlay to determine DF hazards in Jämtland. Quantitative vulnerability assessments involve several decision points (such as the selection of indicators, determination of weights, and summarizing methods) which pose methodological uncertainties. Given that every method option produces a different output, careful consideration is required (Wiréhn et al., 2015). In the same way, determining the level of influence, that is, assigning weights for each parameter needed careful consideration in this thesis. As seen in the worked-out example in Fig. 6, the assigned weights influenced the results of the DF hazard output. Assigning inappropriate weights would lead to incorrect outputs. To avoid this, expert consultation was employed in this study which informed the decision to apply equal weights for all parameters.

Another challenge is ensuring that the parameters are correctly reclassified. Reclassification affects where each item is placed in terms of susceptibility and, consequently, the assigned susceptibility factor. As explained in section 6.3.6 and seen in Fig.6, the weighted overlay tool considers the scores (susceptibility factors) in each cell to determine the score in the resulting outcome cells. Assigning the wrong susceptibility factors would therefore end up in inaccurate hazard classes. To mitigate this, this study extensively consulted experts and literature in the reclassification of the five parameters. Further, the reclassification step was carried out in several iterations where after the initial reclassification, the distribution of the assigned classes was checked against DF tracks in the study area. In cases where previous observations were seen to occur in the lower susceptibility classes, more consultations were made and if necessary, the reclassification was amended. Despite paying utmost care in the reclassification process, this thesis notes some mismatch between the *Very High* DF hazard class and the low correspondence with the SGI and SGU observational datasets (2%, 3%, and 17% for *SGI Problem Areas*, *SGI Mapped High Risks* and *SGU Debris Flow Tracks*, respectively [Table 4]). Probably, the reclassification of the land cover and soil parameters (Table 3; Figs. 9 & 10; Appendices 1 & 2) could have caused this low correspondence. Looking at Fig.10, only 6% and 18% of the classes were considered to have a *Very High* susceptibility to DF hazards for the two parameters (land cover and soil, respectively). In contrast, 53% (land cover) and 81% (soil) of the classes were considered to have a *High* susceptibility to DF hazards. Though there are possible explanations as to how these two parameters (land cover and soil) might have influenced (or failed to influence) DF hazard susceptibility in Jämtland (discussed in section

7.2), future research could try to find a more appropriate way of reclassifying them. Perhaps, the grouping "Silt, Clay, Organic Soils, Others" ought to have been classified as *High* instead of *Very High* while "Sand, Till and Others" ought to have taken the highest susceptibility class (Table 3, Appendix 1). Similarly, for land cover, maybe "Agriculture, Sparse vegetation and Exploited land" (representing *High* susceptibility) could have been included in the *Very High* susceptibility class (Table 3, Appendix 2).

An advantage of iteratively reclassifying the parameters was very apparent for this thesis where based on initial tests on how the parameter classes were distributed, two parameters (planar curvature and profile curvature) were excluded from the study. Profile curvature, which is parallel to the slope, indicates the direction of the maximum slope and influences the surface flow's acceleration and deceleration. This in turn affects erosion and deposition. On the other hand, planar curvature is perpendicular to the direction of the maximum slope and is associated with the flow's convergence and divergence over a surface (Kimerling et al., 2012, as cited by Buckley, n.d.). Putting this into context, for:

- Profile curvature: a negative value indicates that the surface is upwardly convex at that cell (consequently, the flow will be decelerated) while a positive value indicates that the surface is upwardly concave at that cell (consequently, an accelerated flow).
- Planar curvature: a positive value indicates the surface is laterally convex at that cell while a negative indicates lateral concavity at that cell.
- Zero values denote that the surface is linear for both profile and planar curvatures.

For both profile and planar curvature, the number of DF tracks occurring in the "*Very High*" and "*Very Low*" susceptibility classes had an almost equal proportion. That is, about 51% of DF tracks occurred in the "*Very Low*" and 42% in the "*Very High*" [planar curvature] while for profile curvature, "*Very Low*" and "*Very High*" accounted for 48% and 51% of the observations respectively. This almost equal proportion of observations in the extreme classes was an indication that the parameters could have been wrongly classified, clearly demonstrating the complexity of the reclassification exercise and the need to clearly understand how each parameter works. A clarification is made here that no negative impact was noted on the results based on the exclusion of these parameters. Still, this thesis considers curvature parameters as necessary inputs in determining slope instability given that the shape of a slope (concavity or convexity) determines the behavior of surface runoff, which in turn affects the water seepage on a slope, and consequently, ground pore-water pressure (Delmonaco et al., 2003; Sharma, 2013). However, there appears to be a disparity in how curvature values affect slope stability. For example, some studies demonstrated that many DFs occur on concave slopes (as denoted by negative values in planar curvature and positive values in profile curvature) (Delmonaco et al., 2003; Esper Angillieri, 2020; Kanwal et al., 2016; Sharma, 2013). Yet, other studies have demonstrated that DFs still occur on convex slopes (as denoted by positive values in planar curvature and negative ones in profile curvature) (Nohani et al., 2019; Ohlmacher, 2007; Zhuang et al., 2015). Future studies could therefore investigate more to demonstrate how curvature could affect slope stability in Jämtland and consider including the parameter in slope stability investigations for the study area.

## 8. Conclusions

Jämtland County is a national risk area in Sweden when it comes to slope instability and recently (during the summer of 2023), a debris flow (DF) occurred in one of the localities, resulting in severe societal impacts. Yet, DFs are understudied in Sweden. Through this thesis, it has been demonstrated that there is a *Medium* to *High* susceptibility to DF hazards in Jämtland County. More specifically, this thesis shows that:

- In Jämtland County, a DF is likely to occur on moderately steep slopes (slope angles between 12-30°) where there is a dense concentration of waterways, and sparse vegetation and in areas where the land is disturbed due to anthropogenic activities.
- Northern Jämtland (which includes the areas of Ankarvattnet, Viken, Gäddede, and Valsjöbyn) and the western parts (Bakvattnet, Kallsedet, Åre, Duved, Undersåker, and Storlien) are more susceptible to DF hazards.
- 55% and 31% of Jämtland's area is within the *Medium* and *High* hazard classes respectively.
- The study results align with observational datasets from expert organisations (SGI and SGU) where the highest proportion of observations lie between the *Medium* and *High* DF hazard classes. Additionally, negligible observations are found in the lower classes (*Low* and *Very Low*) across the three observational datasets. For the SGI datasets, between 2-3% of observations are within the *Very High* class while in the SGU dataset, 17% of observations are accounted for in the same class.
- 89% of all critical infrastructures included in the analysis are located in areas with *Medium-High* risk exposure.

By mapping DF hazard susceptibility and assessing conditions under which a DF could occur, this study contributes to the much-needed research on DFs in Sweden. This is by demonstrating the processes affecting DF initiation in the study area, and also, by showing where DFs could happen. Furthermore, by analysing the risk exposure of critical infrastructure to DF hazards in the study area, this thesis illustrates the possible impacts on society in a DF event. Apart from directly impacting the exposed critical infrastructure, these consequences can cascade thus affecting lives and livelihoods. The results from this study can hence be used as a foundation for further research. Lastly, this study's methodology can be replicated in other areas in Sweden that might be problematic with DF hazards, therefore, supporting efforts to build knowledge on DFs in Sweden.

The lack of defined criteria on how DF susceptibility parameters should be incorporated in determining DF hazards remains a challenge. This becomes more challenging when data is unavailable for susceptibility parameters believed key for a given study. For example, this study could not obtain data on short-duration rainfall for the study area, and therefore, precipitation as a DF susceptibility parameter, was assumed to be present. Lastly and possibly a major challenge, is ensuring accuracy during the reclassification of DF susceptibility parameters and assigning weights (levels of influence) to each parameter.

Following the outcome of this thesis, it is recommended that:

- Detailed stability investigations and quantifications of DF hazards in the study area should be conducted. Apart from the DF hazard distribution covered in this thesis, such quantifications should entail the magnitude and the scale of DF hazards.
- A vulnerability assessment should be performed to determine the coping and adaptive capacity of the exposed critical infrastructure in the study area.

- Future research needs to develop a criterion for DF susceptibility parameters. Such criterion would for example give the mandatory parameters that must be included, also, the ideal number of parameters that should be considered for DF hazard investigations.
- Specific to the study area, future research could come up with a more suitable way of reclassifying the land cover and soil type parameters. That is, establish a better fit for the levels of influence from the different classes in influencing DF initiation.
- Lastly, worth investigating is land cover and land use changes over time in the study area and how these changes could have an impact on DF hazards. Closely tied to this is the interplay between climate change and anthropogenic activities and how this affects DF hazards. Here, investigations could question how anthropogenic activities over time (for example clear-cutting or agriculture) have influenced precipitation patterns and precipitation intensities and, consequently, debris flows.

## 9. Acknowledgments

First and foremost, I am extremely grateful to my main supervisor, Lotten Wiréhn, and co-supervisor, Robin Blomdin, for their continuous support throughout my thesis. Their dedication, immense knowledge, constructive feedback, insightful suggestions, and mentorship were invaluable for my thesis.

Next, my sincere gratitude goes to Jim Hedfors (Statens Geotekniska Institut-SGI) for availing most of the data used in this study and helping me make sense of this data. Also, his expertise in slope stability, more so in the study area, was incredibly useful. In addition, I am very grateful to Colby Smith (Sveriges Geologiska Undersökning - SGU) for facilitating the use of the SGU dataset.

I greatly appreciate Gustaf Peterson Becher (Sveriges Geologiska Undersökning -SGU) and Christoph Graf (Swiss Federal Institute for Forest, Snow, and Landscape Research) for allowing me to reuse their work. Their photographs were very practical in explaining the technical concepts in this thesis. Also, great thanks to Austin Karani who took his time to produce one of the pictures used in this study.

Lastly, I am deeply indebted to my partner, son, parents, and all my family and friends who have played a role throughout my education and during my thesis. Thank you for your prayers, love, encouragement, and unwavering support.

## 10. References

- Abbaszadeh Shahri, A., Spross, J., Johansson, F., & Larsson, S. (2019). Landslide susceptibility hazard map in southwest Sweden using artificial neural network. *CATENA*, 183, 104225. <https://doi.org/10.1016/j.catena.2019.104225>
- Allaby, M. (2013). *Dictionary of Geology and Earth Sciences (Fourth Edition)*. OUP Oxford.
- Blomdin, R., & Smith, C. (2021). Slamströmssystematik (35-2084/2021). Sveriges Geologiska Undersökning (SGU).
- Brooks, N., Neil Adger, W., & Mick Kelly, P. (2005). The determinants of vulnerability and adaptive capacity at the national level and the implications for adaptation. *Global Environmental Change*, 15(2), 151–163. <https://doi.org/10.1016/j.gloenvcha.2004.12.006>
- Buckley, A. (n.d.). Understanding curvature rasters. ArcGIS Blog. Retrieved March 27, 2024, from <https://www.esri.com/arcgis-blog/products/product/imagery/understanding-curvature-rasters/>
- Casagrande, A. (1948). Unified Soil Classification System. Federal Aviation Administration.
- Coussot, P., & Meunier, M. (1996). Recognition, classification and mechanical description of debris flows. *Earth-Science Reviews*, 40(3), 209–227. [https://doi.org/10.1016/0012-8252\(95\)00065-8](https://doi.org/10.1016/0012-8252(95)00065-8)
- Delmonaco, G., Leoni, G., Margottini, C., Puglisi, C., & Spizzichino, D. (2003). Large scale debris-flow hazard assessment: A geotechnical approach and GIS modelling. *Natural Hazards and Earth System Sciences*, 3(5), 443–455. <https://doi.org/10.5194/nhess-3-443-2003>
- Esper Angillieri, M. Y. (2020). Debris flow susceptibility mapping using frequency ratio and seed cells, in a portion of a mountain international route, Dry Central Andes of Argentina. *CATENA*, 189, 104504. <https://doi.org/10.1016/j.catena.2020.104504>
- Fischer, L., Rubensdotter, L., Sletten, K., Stalsberg, K., Melchiorre, C., Horton, P., & Jaboyedoff, M. (2012a). Debris flow modeling for susceptibility mapping at regional to national scale in Norway.
- Fischer, L., Rubensdotter, L., Sletten, K., Stalsberg, K., Melchiorre, C., Horton, P., & Jaboyedoff, M. (2012b, June 1). Debris flow modeling for susceptibility mapping at regional to national scale in Norway.
- Government of Sweden. (2007). The Consequences of Climate Change and Extreme Weather Events. In *Sweden facing climate change*. Ministry of the Environment. <https://www.government.se/contentassets/5f22ceb87f0d433898c918c2260e51aa/sweden-facing-climate-change-chapter-4-sou-200760/>
- Government Offices of Sweden, M. of the E. (2022). Sweden's Adaptation Communication 2022 [A report to the United Nations Framework Convention on Climate Change November 2022]. Government Offices of Sweden, Ministry of the Environment. [https://unfccc.int/sites/default/files/ACR/2022-11/ADCOM\\_Sweden\\_November\\_221114.pdf](https://unfccc.int/sites/default/files/ACR/2022-11/ADCOM_Sweden_November_221114.pdf)
- Gregoretti, C., Degetto, M., & Boreggio, M. (2016). GIS-based cell model for simulating debris flow runoff on a fan. *Journal of Hydrology*, 534, 326–340. <https://doi.org/10.1016/j.jhydrol.2015.12.054>
- Hawchar, L., Naughton, O., Nolan, P., Stewart, M. G., & Ryan, P. C. (2020). A GIS-based framework for high-level climate change risk assessment of critical infrastructure. *Climate Risk Management*, 29, 100235. <https://doi.org/10.1016/j.crm.2020.100235>
- IPCC. (2019). Annex I: Glossary [Weyer, N.M. (ed.)]. In *IPCC Special Report on the Ocean and Cryosphere in a Changing Climate* [H.-O. Pörtner, D.C. Roberts, V. Masson-

- Delmotte, P. Zhai, M. Tignor, E. Poloczanska, K. Mintenbeck, A. Alegría, M. Nicolai, A. Okem, J. Petzold, B. Rama, N.M. Weyer (eds.)) (pp. 677–702). Cambridge University Press. <https://doi.org/10.1017/9781009157964>
- IPCC. (2022). : Impacts, Adaptation and Vulnerability. Contribution of Working Group II to the Sixth Assessment Report of the Intergovernmental Panel on Climate Change [H.-O. Pörtner, D.C. Roberts, M. Tignor, E.S. Poloczanska, K. Mintenbeck, A. Alegría, M. Craig, S. Langsdorf, S. Löschke, V. Möller, A. Okem, B. Rama (eds.)]. (1st ed.). Cambridge University Press. <https://doi.org/10.1017/9781009325844>
- IPCC. (2023). Contribution of Working Groups I, II and III to the Sixth Assessment Report of the Intergovernmental Panel on Climate Change [Core Writing Team, H. Lee and J. Romero (eds.)]. In *Climate Change 2023: Synthesis Report* (First, pp. 35–115). Intergovernmental Panel on Climate Change (IPCC). <https://doi.org/10.59327/IPCC/AR6-9789291691647>
- Iverson, R. M. (1997). The physics of debris flows. *Reviews of Geophysics*, 35(3), 245–296. <https://doi.org/10.1029/97RG00426>
- Iverson, R. M. (2014). Debris flows: Behaviour and hazard assessment. *Geology Today*, 30(1), 15–20. <https://doi.org/10.1111/gto.12037>
- Jakob, M. (2005). A size classification for debris flows. *Engineering Geology*, 79(3), 151–161. <https://doi.org/10.1016/j.enggeo.2005.01.006>
- Johnsson, I., & Balström, T. (2021). A GIS-based screening method to identify climate change-related threats on road networks: A case study from Sweden. *Climate Risk Management*, 33, 100344. <https://doi.org/10.1016/j.crm.2021.100344>
- Johansson, M. (2015). Data sources on small-scale disaster losses and response – A Swedish case study of extreme rainfalls 2000–2012. *International Journal of Disaster Risk Reduction*, 12, 93–101. <https://doi.org/10.1016/j.ijdr.2014.12.004>
- Kalantari, Z., Nickman, A., Lyon, S. W., Olofsson, B., & Folkesson, L. (2014). A method for mapping flood hazard along roads. *Journal of Environmental Management*, 133, 69–77. <https://doi.org/10.1016/j.jenvman.2013.11.032>
- Kanwal, S., Atif, S., & Shafiq, M. (2016). GIS based landslide susceptibility mapping of northern areas of Pakistan, a case study of Shigar and Shyok Basins. *Geomatics, Natural Hazards and Risk*, 8, 1–19. <https://doi.org/10.1080/19475705.2016.1220023>
- Kneisel, C., Rothenbühler, C., Keller, F., & Haerberli, W. (2007). Hazard assessment of potential periglacial debris flows based on GIS-based spatial modelling and geophysical field surveys: A case study in the Swiss Alps. *Permafrost and Periglacial Processes*, 18(3), 259–268. <https://doi.org/10.1002/ppp.593>
- Koks, E. E., van Ginkel, K. C. H., van Marle, M. J. E., & Lemnitzer, A. (2022). Brief communication: Critical infrastructure impacts of the 2021 mid-July western European flood event. *Natural Hazards and Earth System Sciences*, 22(12), 3831–3838. <https://doi.org/10.5194/nhess-22-3831-2022>
- Länsstyrelsen Jämtlands län. (2020). Regional risk- och sårbarhetsanalys: Jämtlands län 2020 [Sammanställt av Björn Oskarsson]. (451-8771–20). Länsstyrelsen i Jämtlands län. <https://www.lansstyrelsen.se/download/18.1aa62c5318a5efb31adac11/1694084978938/Regional%20risk-%20och%20s%C3%A5rbarhetsanalys%20J%C3%A4mtlands%20l%C3%A4n%202020.pdf>
- Larsson, A., & Große, C. (2023). Data use and data needs in critical infrastructure risk analysis. *Journal of Risk Research*, 26(5), 524–546. <https://doi.org/10.1080/13669877.2023.2181858>

- Li, Y., & Duan, W. (2024). Decoding vegetation's role in landslide susceptibility mapping: An integrated review of techniques and future directions. *Biogeotechnics*, 2(1), 100056. <https://doi.org/10.1016/j.bgtech.2023.100056>
- Liang, Z., Wang, C., Han, S., Ullah Jan Khan, K., & Liu, Y. (2020). Classification and susceptibility assessment of debris flow based on a semi-quantitative method combination of the fuzzy C-means algorithm, factor analysis and efficacy coefficient. *Natural Hazards and Earth System Sciences*, 20(5), 1287–1304. <https://doi.org/10.5194/nhess-20-1287-2020>
- Lindberg, F., Olvmo, M., & Bergdahl, K. (2011). Mapping areas of potential slope failures in cohesive soils using a shadow-casting algorithm – A case study from SW Sweden. *Computers and Geotechnics*, 38(6), 791–799. <https://doi.org/10.1016/j.compgeo.2011.05.003>
- McNamee, M., Pagnon Eriksson, C., Wahlqvist, J., & Johansson, N. (2022). A methodology for assessing wildfire hazard in Sweden – The first step towards a multi-hazard assessment method. *International Journal of Disaster Risk Reduction*, 83, 103415. <https://doi.org/10.1016/j.ijdr.2022.103415>
- Mekonen, A., Raghuvanshi, T., Suryabagavan, K., & Kassawmar, T. (2022). GIS-based landslide susceptibility zonation and risk assessment in complex landscape: A case of Beshilo watershed, northern Ethiopia. 100586. <https://doi.org/10.1016/j.envc.2022.100586>
- MSB. (2012). Guide to risk and vulnerability analyses (Guide MSB366). Swedish Civil Contingencies Agency (MSB).
- MSB. (2014). Action Plan for the Protection of Vital Societal Functions & Critical Infrastructure. Swedish Civil Contingencies Agency (MSB). <https://www.msb.se/siteassets/dokument/publikationer/english-publications/action-plan-for-the-protection-of-vital-societal-functions--critical-infrastructure.pdf>
- Nandi, A., & Shakoor, A. (2010). A GIS-based landslide susceptibility evaluation using bivariate and multivariate statistical analyses. *Engineering Geology*, 110(1), 11–20. <https://doi.org/10.1016/j.enggeo.2009.10.001>
- Nelson, S. (2013). Slope Stability, Triggering Events, Mass Movement Hazards. [https://www2.tulane.edu/~sanelson/Natural\\_Disasters/slopestability.htm](https://www2.tulane.edu/~sanelson/Natural_Disasters/slopestability.htm)
- Niu, C., Wang, Q., Chen, J., Zhang, W., Xu, L., & Wang, K. (2015). Hazard Assessment of Debris Flows in the Reservoir Region of Wudongde Hydropower Station in China. *Sustainability*, 7(11), Article 11. <https://doi.org/10.3390/su71115099>
- Nohani, E., Moharrami, M., Sharafi, S., Khosravi, K., Pradhan, B., Pham, B. T., Lee, S., & M. Melesse, A. (2019). Landslide Susceptibility Mapping Using Different GIS-Based Bivariate Models. *Water*, 11(7), Article 7. <https://doi.org/10.3390/w11071402>
- Nseka, D., Kakembio, V., Mugagga, F., Semakula, H., Opedes, H., Wasswa, H., Ayesiga, P., Nseka, D., Kakembio, V., Mugagga, F., Semakula, H., Opedes, H., Wasswa, H., & Ayesiga, P. (2022). Implications of Soil Properties on Landslide Occurrence in Kigezi Highlands of South Western Uganda. In *Landslides*. IntechOpen. <https://doi.org/10.5772/intechopen.99865>
- Nyberg, R., & Rapp, A. (1998). Extreme Erosional Events and Natural Hazards in Scandinavian Mountains. *Ambio*, 27(4), 292–299.
- Ohlmacher, G. C. (2007). Plan curvature and landslide probability in regions dominated by earth flows and earth slides. *Engineering Geology*, 91(2), 117–134. <https://doi.org/10.1016/j.enggeo.2007.01.005>
- Planeringskatalogen. Swedish power grid. (2022). [https://ext-geodatakatalog-forv.lansstyrelsen.se/PlaneringsKatalogen/GetMetaDataById?id=5b94e98e-9492-404a-84a1-5efab0c87599\\_C&showmetadataview](https://ext-geodatakatalog-forv.lansstyrelsen.se/PlaneringsKatalogen/GetMetaDataById?id=5b94e98e-9492-404a-84a1-5efab0c87599_C&showmetadataview)

- Qin, S., Lv, J., Cao, C., Ma, Z., Hu, X., Liu, F., Qiao, S., & Dou, Q. (2019). Mapping debris flow susceptibility based on watershed unit and grid cell unit: A comparison study. *Geomatics, Natural Hazards and Risk*, 10(1), 1648–1666. <https://doi.org/10.1080/19475705.2019.1604572>
- Rapp, A. (1995). Case Studies of Geoprocesses and Environmental Change in Mountains of Northern Sweden. *Geografiska Annaler. Series A, Physical Geography*, 77(4), 189–198. <https://doi.org/10.2307/521328>
- Rapp, A., & Nyberg, R. (1981). Alpine Debris Flows in Northern Scandinavia. Morphology and Dating by Lichenometry. *Geografiska Annaler. Series A, Physical Geography*, 63(3/4), 183–196. <https://doi.org/10.2307/520831>
- Reisinger, A., Howden, M., & Vera, C. (2020). The Concept of Risk in the IPCC Sixth Assessment Report: A Summary of Cross-Working Group Discussions. Intergovernmental Panel on Climate Change, Geneva, Switzerland.
- Rheinberger, C. M., Romang, H. E., & Bründl, M. (2013). Proportional loss functions for debris flow events. *Natural Hazards and Earth System Sciences*, 13(8), 2147–2156. <https://doi.org/10.5194/nhess-13-2147-2013>
- Rickenmann, D. (1999). Empirical Relationships for Debris Flows. *Natural Hazards*, 19(1), 47–77. <https://doi.org/10.1023/A:1008064220727>
- Rydén Sonesson, T., Johansson, J., & Cedergren, A. (2021). Governance and interdependencies of critical infrastructures: Exploring mechanisms for cross-sector resilience. *Safety Science*, 142, 105383. <https://doi.org/10.1016/j.ssci.2021.105383>
- SCB. (2023). Population in the country, counties and municipalities on 31 December 2023 and Population Change in 2023. Statistikmyndigheten SCB. <https://www.scb.se/en/finding-statistics/statistics-by-subject-area/population/population-composition/population-statistics/pong/tables-and-graphs/population-statistics---year/population-in-the-country-counties-and-municipalities-on-31-december-2023-and-population-change-in-2023/>
- SGI. (2005). Stability and run-off conditions: Guidelines for detailed investigation of slopes and torrents in till and coarse-grained sediments [Written by Karin Rankka and Jan Fallsvik] (68; p. Linköping, Sweden). Statens Geotekniska Institut (SGI).
- SGI. (2024). Investigations of areas subjected to debris flow. Hedfors J. *Personal communication*.
- SGI & MSB. (2021). Riskområden för ras, skred, erosion och översvämning, Redovisning av regeringsuppdrag enligt regeringsbeslut M2019/0124/K1 (10197; p. 204). Statens geotekniska institut, SGI, Linköping och Myndigheten för samhällsskydd och beredskap, MSB, Karlstad. <https://www.msb.se/siteassets/dokument/om-msb/vart-uppdrag/regeringsuppdrag/2021/ru-riskomraden.pdf>
- SGU. (2021). Handledning för jordartsgeologiska kartor och databaser över Sverige [Skriven av Cecilia Karlsson, Gustav Sohlenius & Gustaf Peterson Becher] (2021:17). Sveriges Geologiska Undersökning (SGU).
- SGU. (2023). Dokumentationsrapport. Observationer i samband med slamströmmen i Mörviksån, Åre, 7–8 augusti 2023 [Gustaf Peterson Becher]. <https://resource.sgu.se/dokument/publikation/sgurapport/sgurapport202311rapport/s2311-rapport.pdf>
- SGU. (2024). Debris flow tracks (work in progress). Smith, C.A. *Personal communication*.
- Sharma, R. H. (2013). Evaluating the effect of slope curvature on slope stability by a numerical analysis. *Australian Journal of Earth Sciences*, 60(2), 283–290. <https://doi.org/10.1080/08120099.2013.762942>

- SMHI. (2015). Framtidsklimat i Jämtlands län– enligt RCP-scenarier [ Linda Nylén, Magnus Asp, Steve Berggreen-Clausen, Gitte Berglöv, Emil Björck, Jenny Axén, Mårtensson, Alexandra Ohlsson, Håkan Persson and Elin Sjökvist] (KLIMATOLOGI Nr 34, 2015). Swedish Meteorological and Hydrological Institute (SMHI).
- SMHI. (2023). Jämtland's climate | SMHI. <https://www.smhi.se/kunskapsbanken/klimat/klimatet-i-sveriges-landskap/jamtlands-klimat-1.4996>
- Stroeven, A. P., Hättestrand, C., Kleman, J., Heyman, J., Fabel, D., Fredin, O., Goodfellow, B. W., Harbor, J. M., Jansen, J. D., Olsen, L., Caffee, M. W., Fink, D., Lundqvist, J., Rosqvist, G. C., Strömberg, B., & Jansson, K. N. (2016). Deglaciation of Fennoscandia. *Quaternary Science Reviews*, 147, 91–121. <https://doi.org/10.1016/j.quascirev.2015.09.016>
- Süzen, M. L., & Doyuran, V. (2004). Data driven bivariate landslide susceptibility assessment using geographical information systems: A method and application to Asarsuyu catchment, Turkey. *Engineering Geology*, 71(3), 303–321. [https://doi.org/10.1016/S0013-7952\(03\)00143-1](https://doi.org/10.1016/S0013-7952(03)00143-1)
- Svenska Kraftnät. (2023). Book on Dams: The Swedish Experience. [https://www.svk.se/siteassets/3.sakerhet-och-beredskap/dammsakerhet/vagledning-och-stod/book\\_on\\_dams.pdf](https://www.svk.se/siteassets/3.sakerhet-och-beredskap/dammsakerhet/vagledning-och-stod/book_on_dams.pdf)
- Vianello, D., Vagnon, F., Bonetto, S., & Mosca, P. (2023). Debris flow susceptibility mapping using the Rock Engineering System (RES) method: A case study. *Landslides*, 20(4), 735–756. <https://doi.org/10.1007/s10346-022-01985-6>
- Wiréhn, L., Danielsson, Å., & Neset, T.-S. S. (2015). Assessment of composite index methods for agricultural vulnerability to climate change. *Journal of Environmental Management*, 156, 70–80. <https://doi.org/10.1016/j.jenvman.2015.03.020>
- Xu, W., Yu, W., Jing, S., Zhang, G., & Huang, J. (2013). Debris flow susceptibility assessment by GIS and information value model in a large-scale region, Sichuan Province (China). *Natural Hazards*, 65(3), 1379–1392. <https://doi.org/10.1007/s11069-012-0414-z>
- Zhuang, J., Peng, J., Iqbal, J., Liu, T., Liu, N., Li, Y., & Ma, P. (2015). Identification of landslide spatial distribution and susceptibility assessment in relation to topography in the Xi'an Region, Shaanxi Province, China. *Frontiers of Earth Science*, 9(3), 449–462. <https://doi.org/10.1007/s11707-014-0474-3>
- Zimmermann, M. (1990). Debris flows 1987 in Switzerland: Geomorphological and meteorological aspects. IAHS Publications, 194.

# 11. Appendices

## Appendix 1

Soil parameter

Original classes (as per the study data)	Translation	Reclassification	Susceptibility Classification	Susceptibility factor	Group name
Glaciär	Glaciar	Others	Very low	1	Others
Vatten	Water	Others	Very low	1	
Fyllning	Artificial_Fill	Others	Very Low	1	
Oklassat område, tidvis under vatten	Unclassified_below_water	Others	Very low	1	
Älvsediment sten--block	FluvialSediment_boulders	Boulders	Low	2	Boulders
Blockmark	Boulder_Rich_Soil	Boulders	Low	2	
Isälvsediment, sten--block	Glacialfluvial	Boulders	Low	2	
Svämsediment	Flood_sediment	Others	Medium	3	Gravel, others
Älvsediment, grus	FluvialSedimet_gravel	Gravel	Medium	3	
Älvsediment	FluvialSediment	Gravel	Medium	3	
Isälvsediment, grus	Glaciofluvial_gravel	Gravel	Medium	3	
Isälvsediment	Glacial sediments	Others	Medium	3	
Klapper	Pebbles	Gravel	Medium	3	
Oklassat område	Unclassified	Others	Medium	3	
Postglacial sand--grus	Postglacial sand--gravel	Gravel	Medium	3	
Svallsediment, grus	Wavewashed_gravel	Gravel	Medium	3	
Berg Bedrock	Mountain bedrock	Others	High	4	Sand, Till, Others
Berg	Mountain	Others	High	4	
Rösberg	Weathered_bedrock	Others	High	4	
Sedimentärt berg	Sedimentary_bedrock	Others	High	4	
Rösberg	Weathered_bedrock	Others	High	4	
Vitringsjord	Weathering_soil	Others	High	4	
Isälvsediment, sand	Glaciofluvial_sand	Sand	High	4	
Älvsediment, grovsilt--finsand	FluvialSediment_CoarseSilt_FineSand	Sand	High	4	
Älvsediment, sand	Fluvial Sedimet_sand	Sand	High	4	
Älvsediment, sand	River sediment, sand	Others	High	4	
Bleke och kalkgyttja	Calcium_Rich_Soil	Sand	High	4	
Flygsand	Eolian_Sand	Sand	High	4	
Glacial grovsilt--finsand	Glacial_Coarse_Silt_and_FineSand	Sand	High	4	
Isälvsediment	Glaciofluvial_sediment	Sand	High	4	
Postglacial sand	Postglacial sand	Sand	High	4	
Svämsediment, grovsilt--finsand	Flood_sediment_coarsegrained	Sand	High	4	
Svämsediment, sand	FloodSediment_Sand	Sand	High	4	
Morän omväxlande med sorterade sediment	Till_mixed_with_glaciofluvial_sediment	Till	High	4	
Morän	Till	Till	High	4	

Talus (rasmassor)	Talus	Others	Very High	5	Silts, Clay, Organic Soils Others
Mossetorv	Peat	Organic soils	Very high	5	
Torv, tidvis under vatten	Peat_sometimes_under_water	Organic soils	Very high	5	
Torv	Peat	Organic soils	Very high	5	
Älvsediment, ler--silt	Fluvial Sediment_claySilt	Silt/clay	Very high	5	
Flytjord eller skredjord	Soil_Slope_Processes	Others	Very high	5	
Glacial silt	Glacial silt	Silt/clay	Very high	5	
Gyttja	Mud	Silt/clay	Very high	5	
Gyttjelera (eller lergyttja)	Mud_with_clay	Silt/clay	Very high	5	
Lera	Lera_Clay	Silt/clay	Very high	5	
ler--silt_FloodSediment	FloodSediment_Clay_silt	Silt/clay	Very high	5	
Moränlera eller lerig morän	Moraine clay or muddy moraine	Till	Very high	5	
Postglacial silt	Postglacial silt	Silt/clay	Very high	5	
Silt	Silt	Silt/clay	Very high	5	
Slamströmssediment	DebrisFlow_sediment	Others	Very high	5	
Svämsediment	Swimming sediments, clay--silt	Silt/clay	Very high	5	

## Appendix 2

### Landcover parameter

Original classes (as per the study data)	Translation	Re-classification	Susceptibility Classification	Susceptibility factor	Group name
Öppen våtmark	Open wetland	Wetland	Very Low	1	Wetland, Water, Forested Wetlands
Sjö och vattendrag	Lake and waterways	Water bodies	Very Low	1	
Tallskog (på våtmark)	Pine forest (on wetlands)	Forested wetland	Very Low	1	
Granskog (på våtmark)	Spruce forest (on wetland)	Forested wetland	Very Low	1	
Barrblandskog (på våtmark)	Coniferous mixed forest (on wetlands)	Forested wetland	Very Low	1	
Lövblandad barrskog (på våtmark)	Mixed deciduous coniferous forest (on wetlands)	Forested wetland	Very Low	1	
Triviallövskog (på våtmark)	Deciduous forest (on wetland)	Forested wetland	Very Low	1	
Temporärt ej skog (på våtmark)	Temporarily not forest (on wetland)	Wetland	Very Low	1	
Tallskog (utanför våtmark)	Pine forest_outside wetland	Forested area	Low	2	Forested
Granskog (utanför våtmark)	Spruce forest_outside wetland	Forested area	Low	2	
Barrblandskog (utanför våtmark)	Coniferous forest_outside wetland	Forested area	Low	2	
Lövblandad barrskog (utanför våtmark)	Mixed deciduous coniferous forest_outside wetland	Forested area	Low	2	
Triviallövskog (utanför våtmark)	Deciduous forest (outside wetland)	Forested area	Low	2	
Exploaterad mark, byggnad	Exploited land_building	Buildings	Medium	3	Buildings
Exploaterad mark, ej byggnad eller väg/järnväg	Exploited land not building or road/railway	Other exploited land	High	4	Agriculture, Sparse vegetation,
Exploaterad mark, väg/järnväg	Exploited land_road/railway	Roads/railways	High	4	Exploited
Övrig öppen mark med vegetation	Other open land with vegetation	Sparse vegetation	High	4	Land
Åkermark	Arable land	Agriculture	High	4	
Övrig öppen mark utan vegetation	Other open land without vegetation	Bare areas	Very High	5	Bareland
Temporärt ej skog (utanför våtmark)	Temporarily not forest (outside wetland)	Bare areas	Very High	5	